Graphical Abstract

Click here to download high resolution image

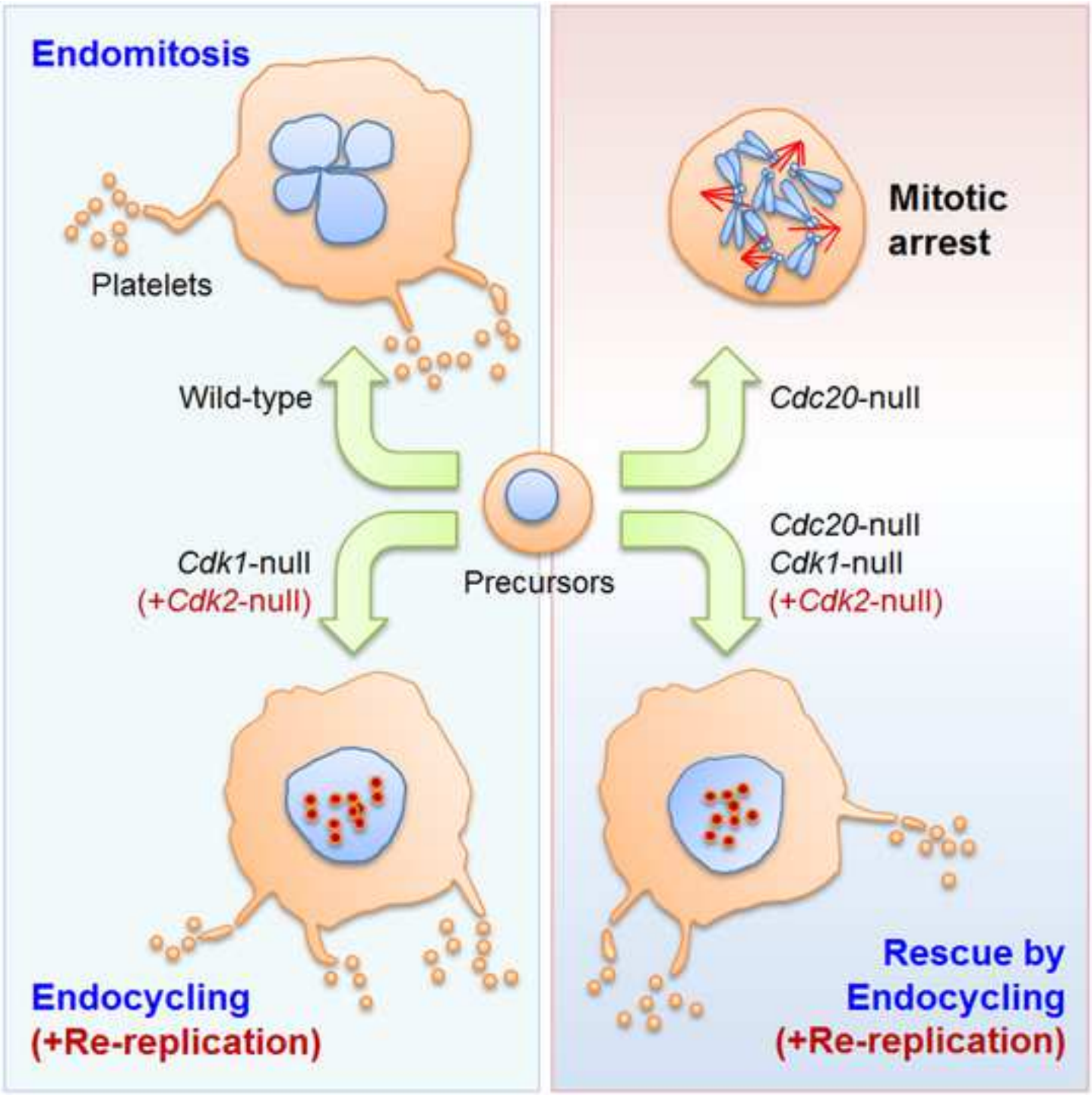

Functional reprogramming of polyploidization in megakaryocytes

Marianna Trakala,[1] Sara Rodríguez-Acebes,[2] María Maroto,[1] Katherine E. Symonds,[3] David Santamaría,[3] Sagrario Ortega,[4] Mariano Barbacid,[3] Juan Méndez[2] and Marcos Malumbres[1,*]

[1] *Cell Division and Cancer Group, Spanish National Cancer Research Centre (CNIO), E-28029 Madrid, Spain*

[2] *DNA Replication Group, CNIO, E-28029 Madrid, Spain*

[3] *Experimental Oncology Group, CNIO, E-28029 Madrid, Spain*

[4] *Transgenic Unit, CNIO, E-28029 Madrid, Spain*

Running title: Functional Reprogramming of polyploidization

Keywords: Anaphase-promoting complex (APC/C)-Cdc20; Cyclin-dependent kinase; Endocycle; Endomitosis; Endoreplication; Platelet formation; Re-replication.

* *Correspondence*: Marcos Malumbres, Centro Nacional de Investigaciones Oncológicas (CNIO), Melchor Fernández Almagro 3, E-28029 Madrid. Tel. +34 91 732 8000; Fax +34 91 732 8033; E-mail: malumbres@cnio.es.

SUMMARY

Polyploidization is a natural process that frequently accompanies differentiation and whose deregulation is linked to genomic instability and cancer. Despite its relevance, why cells select different polyploidization mechanisms is unknown. Here we report a systematic genetic analysis of endomitosis, a process in which megakaryocytes become polyploid by entering mitosis but aborting anaphase. While ablation of the APC/C cofactor Cdc20 results in mitotic arrest and severe thrombocytopenia, lack of the kinases Aurora-B, Cdk1 or Cdk2 does not affect megakaryocyte polyploidization or platelet levels. Ablation of Cdk1 forces a switch to endocycles without mitosis, whereas polyploidization in the absence of Cdk1 and Cdk2 occurs in the presence of aberrant re-replication events. Importantly, ablation of these kinases rescues the defects in Cdc20-null megakaryocytes. These findings suggest that endomitosis can be functionally replaced by alternative polyploidization mechanisms in vivo, and provide the cellular basis for therapeutic approaches aimed to discriminate mitotic and polyploid cells.

HIGHLIGHTS

- Ablation of Cdc20 compromises endomitosis during megakaryocyte polyploidization
- Megakaryocytes can generate platelets in the absence of endomitosis
- Cdk2 is essential to prevent re-replication in the absence of Cdk1 in vivo
- Different polyploidization mechanisms are functionally interchangeable.

INTRODUCTION

Variation in ploidy is commonly found in multiple organisms and polyploid cells are an essential part of the developmental program in many different species (Edgar et al., 2014). In most cases, developmentally programmed polyploidy is an irreversible process linked to terminal cell differentiation and the acquisition of new functional capabilities. In addition, polyploidy has been proposed to buffer the genome against genetic damage (Pandit et al., 2013). Somatic polyploidy can be achieved through multiple modifications of the basic cell division cycle. These special cycles include endocycles, originally described as a process in which rounds of DNA replication occur while mitosis is completely bypassed (successive DNA synthesis and gap phases), or endomitosis, an atypical cell cycle in which cells undergo an aberrant mitosis in the absence of segregation of the previously duplicated genomes. The term "endoreplication" is often used either to refer to endocycles or more widely to include diverse polyploidization mechanisms and will not be used here to avoid confusion. Both endocycles and endomitosis lead to uniform and integral duplication of the genome in mammals (Sher et al., 2013). Other processes, such as re-replication, lead to non-uniform increased ploidy, as a consequence of alteration in the regulatory modules that impose a single round of DNA replication per cell cycle, and normally lead to cell death (Arias and Walter, 2007).

Polyploidization is an essential part of the programmed developmental process required for the formation of placental trophoblast giant cells, which use endocycles to achieve chromatin-values (C-value, a multiple of the DNA content of the unreplicated haploid chromosome complement) of >1000. Similarly, bone marrow megakaryocytes can reach up to 128C in humans or 64C in the mouse through endomitotic cell cycles. Whereas

endocycling is characterized by low expression of mitotic genes, and low cyclin-dependent kinase (Cdk) activity, mitotic genes are normally expressed during endomitosis in megakaryocytes (Edgar and Orr-Weaver, 2001; Sher et al., 2013). Megakaryocytes are the largest (50-100 μm) cells in the bone marrow and they produce platelets by fractionation of the cytoplasm after a terminal differentiation process in which the cytoplasmic volume increases in parallel with ploidy (Thon and Italiano, 2012). Polyploidization in megakaryocytes occurs in the presence of an aberrant mitosis in which cells do not undergo cleavage furrow formation after the 4N stage, and they skip late anaphase and cytokinesis, suggesting that segregation of chromosomes is not necessary for megakaryocyte maturation and platelet formation (Geddis et al., 2007; Kaushansky, 2008; Lordier et al., 2008; Ravid et al., 2002; Wen et al., 2009). The increase in cell volume likely helps to generate a large amount of mRNA and protein necessary to be packaged into platelets (Zimmet and Ravid, 2000). To what extent ploidy and platelet formation are linked is not well established (Machlus and Italiano, 2013), and why polyploidy in these cells is specifically achieved through abortive mitosis is presently unclear.

The variation in polyploidization mechanisms raises the question of whether these unconventional cycles have functional links with the differentiation of specific cell types or they simply represent alternative processes to increase ploidy. In addition, inhibition of multiple mitotic kinases such as Aurora A or Aurora B does not impair polyploidization in cultured megakaryocytes (Lordier et al., 2010; Wen et al., 2012), an observation that, while opening new therapeutic opportunities in cancer (Krause and Crispino, 2013), illustrates our limited understanding on how polyploization is modulated. We have analyzed in this work new mouse strains lacking selected key proteins involved in mitotic entry (Cdks;

Figure 1a), mitotic progression (Aurora B) or mitotic exit [the Anaphase-promoting Complex (APC/C) cofactor Cdc20] during megakaryocyte maturation in vivo. Our results confirm that Aurora B, a kinase essential for proper attachment of microtubules to kinetochores (Nezi and Musacchio, 2009), is not required for megakaryocyte maturation (Lordier et al., 2010). However, genetic ablation of Cdc20 results in mitotic arrest and severe thrombocytopenia indicating that endomitosis is the major megakaryocyte polyploidization mechanism in vivo. Importantly, genetic ablation of Cdk1, an enzyme essential for mitosis, prevents endomitosis but does not impair platelet formation, as a consequence of reprogramming from endomitosis to endocycles that alternate DNA synthesis and gap phases. Similarly, concomitant ablation of Cdk1 and Cdk2 results in aberrant re-replication without dramatically affecting platelet levels. Furthermore, the loss of Cdk1 or the concomitant ablation of both Cdk1 and Cdk2 can significantly rescue proplatelet formation and platelet levels in Cdc20-null mice. These results suggest that reprogramming from endomitosis to other unconventional cell cycles in vivo is compatible with megakaryocyte function, even in the presence of re-replication, a dangerous process in which DNA is unevenly replicated.

RESULTS

Aurora B is dispensable for megakaryocyte development

To understand the requirements for specific mitotic regulators during megakaryocyte development we made use of transgenic mice expressing Cre recombinase under the Platelet factor 4 (Pf4) promoter (Tiedt et al., 2007). In this model Cre is expressed in

megakaryocyte progenitors and mature megakaryocytes with preference for polyploid (≥8C) cells (Figure S1).

Aurora B is a mitotic kinase whose ablation results in a normal mitotic entry but a premature exit from mitosis without being able to segregate chromosomes resulting in tetraploidy (Fernandez-Miranda et al., 2011; Trakala et al., 2013). Specific genetic ablation of the murine *Aurkb* gene in megakaryocytes (Figure S1) resulted in normal survival and no overt defects during development or adulthood of Pf4-Cre; *Aurkb*(Δ/Δ) [from now on *Aurkb*(Δ/Δ)] mice. These mutant mice displayed fully mature megakaryocytes in the bone marrow as indicated by Von Willebrand Factor (VWF) staining (Figure 1b). The absolute number of megakaryocytes and the level of VWF staining per cell was not altered (Figure 1c), and we found no significant differences in the ploidy distribution of cells positive for the megakaryocytic marker CD41 (Figure 1d). In *Aurkb*(Δ/Δ) mice, hematopoietic progenitors displayed normal differentiation kinetics towards CD41+ cells when stimulated with thrombopoietin (TPO), and mature megakaryocytes were able to shed platelets (Figure S1). Accordingly, we found no differences in blood platelet levels in *Aurkb*(Δ/Δ) mice (Figure 1e), indicating a complete maturation, terminal differentiation and full functionality of these mutant megakaryocytes (Figure 1f).

APC/C-Cdc20 is essential for endomitotic exit in megakaryocytes

The APC/C-Cdc20 complex is an E3-ubiquitin ligase whose activity is essential for exiting the mitotic cycle by triggering the degradation of the Cdk1 activator cyclin B1 (Peters, 2006). Thus, Cdc20 ablation does not have any effect in interphase or mitotic entry but cells are trapped in mitosis in the absence of APC/C-Cdc20 activity (Manchado et al.,

2010). Specific genetic ablation of Cdc20 in megakaryocytes (Figure S2) resulted in a dramatic phenotype characterized by lack of mature cells and a significant increase in progenitors and small megakaryocytes in the bone marrow (Figure 2a) and the spleen (Figure S2), a phenotype commonly induced by lack of circulating platelets. *Cdc20*(Δ/Δ) megakaryocytes were characterized by reduced VWF staining (Figure 2a,b) and abundant mitotic figures in the presence of phosphorylated histone H3, suggesting mitotic arrest of mid-size megakaryocytes in the absence of Cdc20 (Figure 2a). In addition, the 16C and 32C populations were almost absent whereas 4-8C megakaryocytes were more abundant (Figure 2a,c), likely as a consequence of the terminal accumulation of mitotic 8C cells as a result of Cdc20 ablation in 2-4C cells. Accordingly, *Cdc20*(Δ/Δ) mutant mice presented severe thrombocytopenia [108.4 ± 70.8 $x10^9$ platelets/L vs. 781.6 ± 171.0 (mean ± SD) in control mice; $p<0.001$; Student's t-test; Figure 2d], thus confirming a critical role for Cdc20 in megakaryocyte function.

We next analyzed the cellular effect of megakaryocyte-specific ablation of Cdc20 using bone marrow progenitors stimulated in vitro with TPO. Three days after stimulation, mutant megakaryocytes were smaller than control cells, presented condensed DNA and were positive for mitotic markers suggesting mitotic arrest in vitro (Figure 2e). We then transduced these megakaryocytes with lentiviral vectors expressing histone H2B fused to the green fluorescent protein (H2B-GFP). As depicted in Figure 2f-h, control *Cdc20*(lox/lox) megakaryocytes underwent typical endomitotic cycles in which cells displayed condensed DNA for about 1-2 h and exited mitosis in the absence of chromosome segregation. Similar assays were performed in Pf4-Cre; *Cdc20*(Δ/Δ); LSL-KFP megakaryocytes in which the activity of Cre resulted in *Cdc20* ablation and the

expression of Katushka fluorescent proteins (KFP) as a result of the excision of a LoxP-STOP-loxP cassette (Figure S1). These *Cdc20*(Δ/Δ) megakaryocytes displayed normal entry into endomitosis but arrested with condensed chromosomes during 10-24 h until cell death (Figure 2g,h). Although we cannot discard another unknown function for Cdc20 in platelet formation, these data are indicative of the essential relevance of Cdc20 during endomitotic exit, resulting in lack of platelets due to mitotic arrest in low-intermediate ploidy Cdc20-null megakaryocytes (Figure 2i).

Cdk1 is essential for endomitosis but dispensable for megakaryopoiesis

By definition, endomitotic cells do enter into mitosis and exit without segregation, whereas endoreplicating cells completely skip mitosis, frequently as a consequence of Cdk1 inhibition (Zielke et al., 2013). We therefore eliminated Cdk1 activity in megakaryocytes to prevent mitotic entry. The resulting Pf4-Cre; *Cdk1*(Δ/Δ) mice did not display major defects in megakaryocyte number, morphology or VWF staining in adult mice (Figure 3a). Similarly, the ratio of highly polyploid (16C-32C) megakaryocytes was partially reduced (Figure 3b), although the number of platelets in peripheral blood was similar to that of control littermates (Figure 3c). Whereas Aurora B and Cdc20 protein levels are controlled by cell cycle-regulated ubiquitin-dependent proteolysis (Peters, 2006), Cdk1 is more stable raising the possibility that its depletion was not efficient in this system. However, we confirmed that Cdk1 protein levels were significantly reduced in mature (>4C) bone marrow *Cdk1*(Δ/Δ) megakaryocytes (Figure 3d). After incubation of bone marrow progenitors with TPO in vitro, *Cdk1*(Δ/Δ) megakaryocytes also accumulated normal levels of ploidy (Figure 3e) and displayed a normal morphology whereas, as a control,

Cdc20(Δ/Δ) megakaryocytes presented smaller nuclei with condensed DNA (Figure 3f). Similar depletion in Cdk1 protein levels was obtained in this assay (Figure 3g). Therefore, the lack of an obvious phenotype in platelet production was not likely due to inefficient ablation of Cdk1 in these genetic models.

To understand the cellular basis of these observations, we monitored polyplodization in *Cdk1*(Δ/Δ) megakaryocyte precursors by time-lapse microscopy. Bone marrow progenitors were transduced with lentiviral vectors expressing lamin-CFP to stain nuclear envelope, and H2B-GFP to label chromatin. In addition, we used a vector expressing geminin-mCherry, a DNA replication regulator induced in S-phase and degraded in an APC/C-dependent manner during mitotic or endomitotic exit (Sakaue-Sawano et al., 2013; Sakaue-Sawano et al., 2008). Using these markers, together with the quantification of nuclear and cellular volumes, endocycles can be readily monitored in wild-type megakaryocytes (Figure S3). Control megakaryocytes were recorded for several days and the behavior of individual cells is depicted in Figure 4a. Most control megakaryocytes were characterized by abortive mitosis (condensed chromosomes and pan-cellular geminin signal, degradation of geminin (geminin^{low} phase) followed in most cases by re-expression of geminin (geminin^{high}) and a new endomitotic phase (Figure 4a-c). The histone signal (Figure S3) and nuclear volume (Figure 4c) similarly increased ~2 fold during the geminin^{high} phase suggesting DNA replication in each of these endocycles. Cell volumes also increased during this process without clearly correlating with any particular phase (Figure 4c).

In most *Cdk1*(Δ/Δ) megakaryocytes, however, geminin was degraded in the absence of endomitosis (Figure 4d-f). In these cells, geminin displayed an exclusive nuclear

localization in agreement with the maintenance of the nuclear envelope (as detected by lamin signal; Figure S4) and the lack of chromosome condensation (as monitored by histone signal; Figure 4e and S4). Yet, geminin was degraded and cells underwent additional cycles characterized by the oscillation in geminin levels in the absence of mitosis. Interestingly, histone H2B-GFP signal (Figure S4) and nuclear volume (Figure 4f) increased about 2-fold in each of these endocycles suggesting the presence of DNA replication throughout the geminin^{high} phase. Due to the difficulties in directly monitoring Cdk1 ablation in these individual cells, we also used the LSL-KFP allele as a surrogate marker for Cre activity. About 70% of Pf4-Cre; *Cdk1*(Δ/Δ); LSL-KFP cells positive for the Katushka signal (an indication of Cre activity in polyploid cells; see Figure S1) underwent cycles in which geminin was degraded in the absence of endomitosis (S-G-S cycles), whereas all control Pf4-Cre; *Cdk1*(+/+); LSL-KFP cells underwent typical endomitotic cycles (Figure S4). The fact that the increase in ploidy was similar in wild-type and *Cdk1*(Δ/Δ) cells (Figure 4c,f) indicates that megakaryocytes are able to polyploidize using endocycling as an alternative route to endomitosis in the absence of Cdk1 (Figure 4g).

Cdk2 prevents re-replication in the absence of Cdk1

We next used Cdk2-deficient mice to test the contribution of this kinase which is highly related to Cdk1 (Malumbres et al., 2009), but whose relevance to somatic cell cycles is not clear due to the lack of mitotic phenotypes in Cdk2-deficient mice (Malumbres and Barbacid, 2009; Ortega et al., 2003). In the absence of Cdk2 (Figure S5) megakaryocytes displayed normal morphology (Figure 5a) and platelet number (943.3 ± 137.6 x10^9 platelets/L versus 852.3 ± 134.4 in wild-type littermates; $p>0.05$, Student t-test). Similarly, lack of Cdk2 did not dramatically alter megakaryocyte maturation (Figure 5a) or platelet

numbers in a *Cdk1*(Δ/Δ) background [739 ± 56.6 x10^9 platelets/L in *Cdk1*(Δ/Δ); *Cdk2*(–/–) versus 863.4 3 ± 179.6 in *Cdk1*(Δ/Δ); *Cdk2*(+/+) littermates; p>0.05, Student t-test]. Unexpectedly, genetic ablation of Cdk2 in a Cdk1-null background resulted in pan-nuclear phosphorylation of H2AX (γH2AX) in megakaryocytes. Whereas γH2AX is usually found in a light, scattered pattern during normal DNA replication, strong pan-nuclear staining is indicative of a response to DNA damage. Wild-type megakaryocytes or cells deficient in Cdk1 or Cdk2 displayed a scattered pattern in about 25% of the cells. However, *Cdk1*(Δ/Δ); *Cdk2*(–/–) megakaryocytes displayed an additional 52% of cells with strong pan-nuclear γH2AX staining suggesting abnormal replication events (Figure 5a,b). These data correlated with abnormal ploidy in *Cdk1*(Δ/Δ); *Cdk2*(–/–) megakaryocytes in which the sharp peaks representing the 8C, 16C and 32C populations were substituted with a continuous distribution of high ploidy cells, a phenotype frequently attributed to re-replication (Figure 5c).

Cdk1(Δ/Δ); *Cdk2*(–/–) megakaryocytes also presented geminin^{low} and geminin^{high} phases without evidences for mitosis in most cases (Figure 5d,e). Interestingly, the duration of many geminin^{high} phases was longer when compared to wild-type or *Cdk1*(Δ/Δ) cells (Figure 5d-g), and the increase in nuclear volume per geminin^{high} phase in *Cdk1*(Δ/Δ); *Cdk2*(–/–) megakaryocytes was higher than 2-fold, and correlated (R^2=0.887) with the length of the individual geminin^{high} phases (Figure 5g). The fact that the increase in nuclear size was higher than expected and did not correspond to discrete genome doublings is consistent with a phenomenon known as re-replication in which the original DNA is copied more than once within each S-phase (Figure 5h).

Cdk1 and Cdk2 ablation rescues platelet defects in the absence of Cdc20

Since inactivation of Cdk1 or Cdk1 plus Cdk2 may trigger polyploidization in the absence of endomitosis, we hypothesized that lack of Cdks could rescue the mitotic-specific defects observed in Cdc20-null megakaryocytes by reprogramming the polyploidization process thus bypassing the mitotic arrest. We therefore generated Pf4-Cre; *Cdc20*(Δ/Δ); *Cdk1*(Δ/Δ) or Pf4-Cre; *Cdc20*(Δ/Δ); *Cdk1*(Δ/Δ); *Cdk2*(–/–) mutant mice. Whereas genetic ablation of Cdc20 was characterized by the presence of small megakaryocytes frequently arrested in mitosis, simultaneous ablation of Cdk1 allowed the accumulation of big megakaryocytes with increased VWF signal (Figure 6a,b) and ploidy (Figure 6c), suggesting a partial rescue in the maturation of these cells. Strikingly, concomitant ablation of Cdk1 and Cdk2 in a Cdc20 background led to an improved rescue in the maturation of megakaryocytes (Figure 6a,b). The rescue in ploidy was also improved since these triple mutant mice displayed clear 16C and 32C peaks in the presence of a significant number of cells with intermediate ploidy content (Figure 6c). These triple mutants displayed clear polyploid peaks what were not as evident in re-replicative *Cdk1*(Δ/Δ); *Cdk2*(–/–) megakaryocytes (Figure 5c). As detected by flow cytometry studies, about 17% of triple mutant cells were positive for the mitotic marker phospho-histone H3, an observation that likely reflects a partial mitotic arrest imposed by lack of Cdc20 in low-ploidy cells that may still express Cdk1 or Cdk2 (Figure S5). Yet, the percentage of cells with intermediate levels of ploidy (different from an exact multiple of the normal diploid number) was increased in *Cdc20*(Δ/Δ); *Cdk1*(Δ/Δ); *Cdk2*(–/–) triple mutants to levels close to those observed in *Cdk1*(Δ/Δ); *Cdk2*(–/–) double mutants (Figure S5). Overall, the percentage of mitotic megakaryocytes was significantly reduced in *Cdc20*(Δ/Δ); *Cdk1*(Δ/Δ) and *Cdc20*(Δ/Δ); *Cdk1*(Δ/Δ); *Cdk2*(–/–) mutant mice

(Figure 6d), suggesting that Cdk1-null or Cdk1;Cdk2-null megakaryocytes were able either to exit from the mitotic arrest imposed by lack of Cdc20, or to polyploidize and form platelets in a endomitotic-independent manner. Time-lapse microscopy analysis indicated that no megakaryocyte was able to exit from the mitotic arrest imposed by Cdc20 ablation as a viable cell (Figure S5). However, about half of viable cells were able to start polyploidization cycles in the absence of mitosis suggesting that maturation of these cells was mediated by alternative polyploidization mechanisms. The reprogramming was also suggested by careful examination of nuclear morphology in vivo. Whereas wild-type (or Cdk2-null) megakaryocytes displayed typical complex nuclei characterized by the presence of multiple lobules (as a result of abortive chromosome segregation), *Cdk1*(Δ/Δ) or *Cdk1*(Δ/Δ); *Cdk2*(–/–) megakaryocytes (either in a wild-type or Cdc20-null background) were frequently mono- or bi-nucleated (Figure 6e), supporting the hypothesis of a polyploidization mechanism different from endomitosis in vivo.

The presence of pan-nuclear staining of γH2AX in *Cdc20*(Δ/Δ); *Cdk1*(Δ/Δ); *Cdk2*(–/–) also indicated replicative defects in triple mutant mice that were not present in *Cdc20*(Δ/Δ); *Cdk1*(Δ/Δ) megakaryocytes (Figure 6a). We therefore tested whether these defects could be due to re-replication in the absence of both Cdk1 and Cdk2 by using an adaptation of DNA fiber spreading assays (Neelsen et al., 2013) to monitor re-replication on single DNA molecules from megakaryocytes. Cells were sequentially incubated with CldU and IdU, a technique commonly used to distinguish moving forks, origin firing and termination events. In this protocol, the overlap in these signals on the same replication track is indicative of re-replication events caused by two or more rounds of activation of the same replication origin. As shown in Figure 7a, the levels of re-replication were below 5%

in wild-type megakaryocytes as well as in Cdk1- or Cdk2-single mutants in agreement with previous data in other control cultures (Dorn et al., 2009; Neelsen et al., 2013). However, about 15-17% of labeled DNA replication tracks from both *Cdk1*(Δ/Δ); *Cdk2*(–/–) and *Cdc20*(Δ/Δ); *Cdk1*(Δ/Δ); *Cdk2*(–/–) megakaryocytes corresponded to re-replication events, indicating a potential loss of control over origin licensing in the absence of these two kinases.

Alternative polyploidy cycles can drive proplatelet and platelet formation

To understand whether megakaryocytes were functional in the presence of alternative polyploidization mechanisms, we next performed proplatelet formation assays ex vivo. Five days after TPO-induced differentiation of bone marrow progenitors, 24 ± 2% (mean ± SEM) of wild-type endomitotic megakaryocytes were able to form proplatelets (Figure 7b). *Cdk1*(Δ/Δ) megakaryocytes displayed a similar percentage of proplatelet-bearing cells (21 ± 2%; Figure 7b,c). As a negative control, only 0.9 ± 0.5% of *Cdc20*(Δ/Δ) megakaryocytes were able to form proplatelets. Importantly, concomitant ablation of Cdk1 in a Cdc20-null background led to a significant rescue of proplatelet formation (7.0 ± 0.4%) and this was further improved in *Cdc20*(Δ/Δ); *Cdk1*(Δ/Δ); *Cdk2*(–/–) triple mutant cultures (16 ± 3.5%; Figure 7b,c).

In agreement with these data, genetic ablation of Cdk1 was able to significantly rescue thrombocytopenia in Cdc20-null mice. The mean number of circulating platelets increased from 114 ± 79 $x10^9$ platelets/L in *Cdc20*(Δ/Δ) animals to 376 ± 18 $x10^9$ platelets/L in *Cdc20*(Δ/Δ); *Cdk1*(Δ/Δ) double mutant mice (Figure 7d). Interestingly, concomitant ablation of one or two alleles of Cdk2 further improved this rescue (598 ± 42

x10^9 platelets/L in *Cdc20*(Δ/Δ); *Cdk1*(Δ/Δ); *Cdk2*(–/–) triple mutants). All together, these results indicate that alternative polyploidization mechanisms can result in functional megakaryocytes in vivo even in the presence of re-replication events (Figure 7e).

DISCUSSION

Polyploidization provides an evolutionarily conserved mechanism for post-mitotic cell growth in unicellular and multicellular organisms (Edgar et al., 2014; Pandit et al., 2013). The increase in ploidy can be achieved by variants of the cell cycle which have been analyzed in detail in *Drosophila* and *Arabidopsis* due to the availability of multiple genetic models (Edgar et al., 2014). In the mouse, polyploidization has been mostly studied in trophoblast giant cells and hepatocytes, two cell types that undergo endocycling or acytokinetic mitosis. In trophoblast giant cells, mitosis is prevented by inhibition of Cdk1 activity by multiple mechanisms such as induction of the $p57^{Kip2}$ Cdk inhibitor, or by enhanced APC/C-Cdh1 activity that results in the ubiquitin-dependent degradation of mitotic cyclins (Garcia-Higuera et al., 2008; Ullah et al., 2008; Zielke et al., 2013).

Early assays in stimulated megakaryocytes in vitro concluded that polyploidization in these cells is achieved by endomitotic cycles in which cells skip the later stages of mitosis and cytokinesis [reviewed in (Ravid et al., 2002)]. Recent data using time-lapse microscopy indicates different dynamics in furrow formation between low- and high ploidy megakaryocytes (Lordier et al., 2008; Papadantonakis et al., 2008). The resulting cells usually display a single polylobulated nucleus as a consequence of chromosome decondensation and nuclear envelope re-formation after aborted anaphase. The fact that more than 80% of mature megakaryocytes arrest in mitosis in the absence of Cdc20 (Figure

2) supports the notion that endomitosis is the major polyploidization mechanism for megakaryocytes in vivo. The requirements for other mitotic regulators are unclear and separate observations in the past suggested contradictory data on the relevance of the expression of several mitotic regulators such as Cdk-cyclin complexes or mitotic regulators during endomitosis (Vitrat et al., 1998; Zhang et al., 1996). Recent data indicate that mature megakaryocytes do not display a major defect in the expression of the mitotic machinery (Sher et al., 2013), although differences in specific RhoA exchange factors or non-muscle myosins may explain defects in furrow formation in high-ploidy megakaryocytes (Gao et al., 2012; Lordier et al., 2012; Lordier et al., 2008). Aurora B, an enzyme essential for error correction during microtubule-kinetochore attachment, is dispensable for megakaryocytes in vivo (Figure 1), in agreement with previous data showing that chemical inhibition of this kinase does not prevent polyploidization and maturation of these cells (Lordier et al., 2010; Wen et al., 2012). Thus, whereas most mitotic genes are expressed in megakaryocytes, some of them may be dispensable due to the lack of ordered separation of chromosomes during mitotic exit.

Here we have found that genetic ablation of Cdk1 results in bypass of mitosis in megakaryocytes (Figures 3 and 4), a process that has also been observed in some cell lines (Hochegger et al., 2007) or in hepatocytes (Diril et al., 2012), a cell-type known to undergo endocycling upon different stress conditions (Gupta, 2000). Importantly, Cdk1-deficient megakaryocytes not only can increase ploidy using endocycles but also generate normal levels of proplatelets in vitro and platelets in vivo (Figures 3,4 and 7).

Unconventional cell cycles such as endomitosis or endocycles maintain a mechanism to enable the oscillation in Cdk and APC/C activity, thus ensuring the periodic re-licensing of DNA for replication. Loss of this control leads to re-replication (also known

as over-replication), a process in which some origins can be re-licensed and re-fired before the whole genome has been duplicated once, resulting in genome compositions that differ from multiples of the normal ploidy (Arias and Walter, 2007). Apart from its physiological role in the amplification of specific genes during the development of the *Drosophila* ovary (Calvi et al., 1998; Claycomb et al., 2004), re-replication is considered an aberrant process that does not appear to occur as part of any developmental program in mammals. Pioneering experiments by Nurse, Nasmyth and colleagues showed that Cdks play a dual role in triggering replication initiation and limiting DNA replication to a single round per cell cycle by inhibiting re-licensing of origins within a single S-phase (Broek et al., 1991; Dahmann et al., 1995). In mammals, both Cdk1 and Cdk2 can prevent the function of the replication complex by phosphorylating multiple regulators such as Cdt1, Cdc6, Orc1 or MCM proteins, or by preventing polymerase activity [reviewed in (Zhu, 2004)]. Depletion of Cdk1 and/or Cdk2 has been linked to re-replication phenomena in cell lines although in many cases these data are confusing given the use of different nomenclature or the lack of direct techniques, such as DNA fiber analysis to monitor these changes. Whereas Cdk1 is essential for the mammalian cell cycle (Diril et al., 2012; Santamaria et al., 2007), Cdk2 ablation in somatic cells does not result in major defects in the mitotic cell cycle, likely as a consequence of compensation by other Cdks (Berthet et al., 2003; Ortega et al., 2003). Interestingly, concomitant ablation of these two Cdks in megakaryocytes results in re-replication events, a phenomenon that cannot be easily repaired and leads to DNA breaks and apoptosis in other cell types (Arias and Walter, 2007; Neelsen et al., 2013). In *Drosophila*, polyploidy occurs in the absence of DNA-damage induced apoptosis (Hassel et al., 2014; Mehrotra et al., 2008). Similarly, megakaryocytes seem to be tolerant to the aberrant ploidy resulting from re-replication, probably as a consequence of the upregulation

of prosurvival proteins to progress safely through proplatelet formation and platelet shedding (Josefsson et al., 2011). Thus, Cdk1;Cdk2-deficient megakaryocytes provide a model for functional re-replication in mammals.

These data also suggest that, although Cdk1 and Cdk2 may eventually participate in triggering DNA replication in mammalian cells (Moore et al., 2003; Santamaria et al., 2007), they are both dispensable for S-phase entry, at least in the presence of other interphase Cdks. Although dispensable for G1/S transition, our work indicates that Cdk2 is essential to prevent re-replication in the absence of Cdk1, an interesting observation given the lack of essential functions for this protein in mammals (Berthet et al., 2003; Malumbres and Barbacid, 2009; Ortega et al., 2003), and the possible use of Cdk1/Cdk2 inhibitors to trigger lethal re-replication in tumor cells.

Strikingly, by modulating Cdk activity in megakaryocytes in vivo, we found that alternative polyploidization mechanisms besides endomitosis can lead to highly polyploid and mature megakaryocytes. The fact that reprogrammed megakaryocytes are functional even in the presence of DNA damage and absence of discrete ploidy peaks (Figure 5), suggests that the major, if not the only, function of polyploidization is to increase cell size for platelet generation (Thon and Italiano, 2012). Since endomitosis is one of the modified cell cycles least variant from the archetypal cell cycle, a simple interpretation suggests that megakaryocytes (which do not reach the higher ploidy levels observed in other cells such as trophoblast giant cells; >1000C) simply select the smaller degeneration of the mitotic cell cycle required for expansion of progenitors to become polyploid. The slight defects in platelet levels in Cdk1- or Cdk1; Cdk2-null mice and the incomplete rescue induced by lack of these kinases in Cdc20-deficient mice may indicate that, although endocycling or re-replication can be functionally used during megakaryocyte polyploidization, they may be

less efficient than endomitosis. As an attractive possibility, it has been recently proposed that the multilobulated nuclei generated during mitosis may participate in the establishment of the forces required for membrane fragmentation during the formation of proplatelets (Eckly et al., 2014).

In addition to its critical role as part of developmental or stress programs, polyploidization can also be a quick route to aneuploidy and genome instability (Davoli and de Lange, 2011; Pandit et al., 2013). Recent data has shown that inhibition of Aurora kinases as well as Cdk1 or Cdk2 in megakaryocytic leukemia cells leads not only to increased ploidy but also to the expression of differentiation markers (Wen et al., 2012). Thus, polyploidization not only accompanies but can actually trigger the differentiation process in megakaryocytes. Since Cdk1 is essential for mitosis in all cells tested, it can be expected that the differentiation process induced by Cdk1 inhibition (Wen et al., 2012) is actually mediated by endocycling rather than endomitosis, although this has not been tested in detail. The fact that mitotic kinases such as Aurora A, Aurora B or Cdk1 are not required for the function of endomitotic or endocycling cells, while being essential for mitotic cell cycles, opens new avenues in the use of inhibitors against these proteins in therapeutic approaches against specific human cancers (Krause and Crispino, 2013).

EXPERIMENTAL PROCEDURES

Mouse colony and histological analysis

Mice deficient in Aurora-B (Fernandez-Miranda et al., 2011), Cdc20 (Manchado et al., 2010) or Cdk2 (Ortega et al., 2003), and the Pf4-Cre (Tiedt et al., 2007) and LSL-Katushka (Dieguez-Hurtado et al., 2011) tool lines have been described previously. See also

Supplemental Experimental Procedures. Expression of Cre in bone marrow cells does not alter polyploidization of megakaryocytes (Wen et al., 2009). The Cdk1 conditionally allele will be reported elsewhere (D.S. and M.B.). Mice were housed in the pathogen-free animal facility of the Centro Nacional de Investigaciones Oncológicas (Madrid) following the animal care standards of the institution. All animal protocols were approved by the local committee for animal care and research. The following antibodies were used for immunohistochemistry in tissue sections: von Willebrand Factor (FVIII, Dako; 1:2000), phospho-histone H3 (Ser10; Millipore; 1:2000) or γ-H2AX (Ser139, Millipore; 1:2000). For quantification, paraffin sections stained with anti-VWF were examined using an Olympus BX51 microscope equipped with objective lenses (40/0.75, 20/0.4, 10/0.25, and 4/0.1). The relative amount of pixels positive for VWF was used as a score.

Cytometry

Flow cytometric analysis of DNA content and surface markers of megakaryocytes was determined by staining either whole bone marrow cells or hematopoietic progenitor cultures from 0-5 days in presence of TPO with fluorescein isothiocyanate (FITC)–conjugated anti-CD41 antibody (BD Biosciences) followed by fixation with 4% PFA at room temperature for 30 min followed by staining with 2 μg/ml DAPI (4,6 diaminophenylindole, Sigma-Aldrich) or 5 μg/ml Hoechst (Sigma-Aldrich) for 1 h. See also Supplemental Experimental Procedures.

Megakaryocyte differentiation and functional assays

Cells from the bone marrow or fetal liver were isolated as indicated in Supplemental Information. Lin^- cells were grown in Dulbecco‟ s modified Eagle's medium (DMEM; Gibco) supplemented with antibiotics and 10% fetal bovine serum (FBS), and stimulated with 50-100 ng/mL murine TPO (PeproTech) at least during 5 days. For functional assays, the cell population was enriched in mature megakaryocytes either by using a 1.5%/3% bovine serum albumin (BSA) gradient under gravity (1*g*) for 45 minutes or by cell sorting using CD41 staining after 4-5 days of culture in the presence of TPO. Proplatelet formation assays were performed essentially as described previously (Bluteau et al., 2014).

Protein analysis and immunofluorescence

For immunodetection in protein lysates, proteins were separated on SDS-PAGE, transferred to nitrocellulose membranes (BioRad), and probed using specific primary antibodies against Cdk1 (Santa Cruz Biotechnology; 1:500) and vinculin (Sigma; 1:3000) as a loading control. For immunofluorescence, cells were fixed with 4% paraformaldehyde in PBS for 10 min at 37ºC, permeabilized with PBS-Triton 0.15% for 2 min at 37ºC, blocked with 3% BSA and subsequently incubated during 1-3 h with the primary antibody against Aurora B (Abcam; 1:200) or α-tubulin (Sigma; 1:2000). Matching secondary antibodies with different Alexa dies (488, 594, 647; Molecular Probes) and DAPI (Prolong Gold antifade; Invitrogen) were used for nuclei visualization. Image acquisition was performed using either a confocal ultra-spectral microscope (Leica TCS-SP5) or a Leica DMI fluorescence 6000B microscope.

Time-lapse microscopy

Cells were transduced with lentiviruses or retroviruses encoding histone H2B-GFP, lamin A-CFP (a gift from V. Andrés, CNIC, Madrid) and geminin-mCherry (Abe et al., 2013). Transduced cells were then plated on eight-well glass-bottom dishes (Ibidi) embedded in methylcellulose containing Iscove's Modified Dulbecco's Medium (IMDM) with 2% Fetal Bovine Serum and 100 ng/mL murine TPO, in order to minimize cell movement. Time-lapse acquisition was performed with a Leica DMI 6000B microscope equipped with a 63×/1.5 N.A. objective lens or DeltaVision RT imaging system (Applied Precision; IX70/71; Olympus) equipped with a Plan Apochromatic 40×/1.42 N.A. objective lens, and maintained at 37 °C in a humidified CO2 chamber. Images were acquired every 7 min for up to 10 days. Quantitative analysis was performed by ImageJ software.

DNA fiber assay

For the analysis of DNA replication in stretched DNA fibers, cells were processed using a protocol modified from (Neelsen et al., 2013). Essentially, cells were incubated in presence of 50 µM CldU (5-Clorodeoxyuridine) for 2 hours and pulsed for 30 min with 250 µM IdU (5-Iododeoxyuridine). One drop containing 500-700 cells was placed on a microscope slide and cells were lysed with the addition of 10 µl lysis buffer [0.5% SDS, Tris (pH 7.4), EDTA 50mM] for 6 min at room temperature. Slides were tilted at a 10-15^{o} angle to allow the DNA suspension to run slowly down the slide. Slides were air-dried and fixed in 3:1 v/v methanol:acetic acid. Following DNA denaturation with 2.5M HCl for 30 min, DNA fibers were washed and blocked with PBS, 1% BSA, 0.1% Triton X-100 and incubated with primary antibodies against CldU and IdU (Abcam and Becton-Dickinson; 1:100). Matching secondary antibodies conjugated to Alexa dyes (488, 594, 647) were used for signal visualization. ssDNA was stained with a specific antibody (anti-ssDNA mouse monoclonal

IgG2a; Millipore) to ensure the analysis of individual fibers. Image acquisition was performed using a Leica DMI fluorescence 6000B microscope. At least 500 replication tracks containing green signal were scored in each condition, and the percentage of re-replication events (yellow tracks) in the total population of green tracks was analyzed.

Statistical analysis

Statistical analysis was carried out using Prism 5 (GraphPad). All statistical tests were performed using two-sided, unpaired Student's t-tests, or the Fisher's exact test. Data with $p < 0.05$ were considered statistically significant. In most figures, *, $p<0.05$; **, $p<0.01$; ***, $p<0.001$.

AUTHOR CONTRIBUTIONS

M.T. performed most cellular and mouse experiments. M.Maroto helped with the quantification of histological samples. M.T., S.R. and J.M. performed re-replication analyses in stretched DNA fibers. C.E.S, D.S. and M.B. generated the *Cdk1*(lox) allele and S.O. generated the Katushka allele. M.Malumbres conceived and supervised the project. M.T. and M.Malumbres analyzed the data and wrote the manuscript.

ACKNOWLEDGEMENTS

We are fully indebted to V. Andrés (CNIC, Madrid, Spain) and A. Miyawaki (RIKEN, Saitama, Japan) for reagents. We thank Ana Pérez for technical help, Lola Martínez and

Diego Megías (CNIO) for help with cytometry and microscopy analysis; members of the Comparative Pathology and Transgenic Units of the CNIO for excellent technical support and Sara Leceta and Sheila Rueda for help with animal management. We also thank Miguel Torres and Guadalupe Sabio (CNIC) for help with blood counters. M.T. received a fellowship from the Foundation La Caixa. This work was funded by grants from the Foundation Ramón Areces, Spanish Ministry of Economy and Competitiveness (MINECO; SAF2012-38215 to M.Malumbres, SAF2010-18765 to S.O., and BFU2010-21467 and CSD2007-00015 to J.M.), the OncoCycle Programme (S2010/BMD-2470 to M.Malumbres and M.B.) from the Comunidad de Madrid, and the European Union Seventh Framework Programme (MitoSys project; HEALTH-F5-2010-241548 to M.Malumbres).

COMPETING FINANCIAL INTERESTS

The authors declare no competing financial interests.

FIGURE LEGENDS

Figure 1. **Aurora-B is dispensable for megakaryopoiesis and platelet formation.**

a) Schematic representation of the role of the molecules discussed in this work during endomitosis.

b) Bone marrow sections from 12 week-old mice were stained with Hematoxylin and Eosin (H&E) or treated for immunohistochemical staining of Von Willebrand Factor (VWF). Scale bars, 50 μm (insets 20 μm).

c) Pf4-Cre; *Aurkb*(Δ/Δ) mice show normal megakaryocyte number (MKs per 40X microscopic field) and VWF staining (relative VWF signal per cell). At least 300 megakaryocytes from three different animals per genotype were counted. Data are mean ± SEM (ns; not significant; $p>0.05$; Student's t-test)

d) Ploidy distribution (after DAPI staining) of CD41+ bone marrow cells.

e) Blood platelet levels from 8-12-week old *Aurkb*(Δ/Δ) and control mice (ns; not significant; $p>0.05$; Student's t-test).

f) Schematic representation of mitotic progression in the absence of Aurora B.

See also Figure S1.

Figure 2. **Cdc20 is essential for megakaryocyte maturation and platelet production.**

a) Hematoxylin and Eosin (H&E) and immunohistochemical staining for Von Willebrand Factor (VWF) and phosphorylation of histone H3 (pH3) in 12 week-old mice. Scale bars, 50 μm (insets, 20 μm). The abundance of megakaryocytes (mean ± SEM megakaryocyte per 40X microscopy field) and the percentage of mitotic cells (mean ± SEM) are indicated in the histograms. n=250 cells from 3 mice per genotype.

b) Quantification of VWF signal in Cdc20-null and control megakaryocytes. n=250 cells from 3 mice per genotype.

c) Ploidy distribution of bone marrow CD41+ cells after DAPI staining.

d) Blood platelet levels from 8-12 week-old *Cdc20*(Δ/Δ) and control.

e) Bone marrow cells were stimulated with TPO for 3 days. Micrographs represent brightfield and Giemsa staining, and immunofluorescence (IF) for Aurora B (red; DAPI is in blue). Scale bars, 50 μm or 20 μm (IF).

f) Cell fate of Cdc20-deficient megakaryocytes. Every row represents a single cell and purple frames depict endomitosis. Time 0 is set to mitotic entry (DNA condensation). Interphase is shown in pale brown and mitosis in black. Cell death is represented by a red circle. Only a control cell (top) is shown as an example.

g) Duration of mitosis (DOM) in minutes estimated by the analysis of individual cells by time-lapse microscopy. In *Cdc20*(Δ/Δ) megakaryocytes, the DOM is considered from DNA condensation until cells die in mitosis.

h) Representative time-lapse images of bone marrow derived megakaryocytes stably expressing histone H2B-GFP (green). The red color in *Cdc20*(Δ/Δ) megakaryocytes corresponds to Katushka fluorescent protein (KFP) which is expressed in a Cre-dependent manner.

i) Scheme representing the essential role of Cdc20 for endomitotic exit in megakaryocytes. The Student's t-test was used for statistics in a), b), d) and g). ***, $p<0.001$.

See also Figure S2.

Figure 3. **Normal megakaryocyte function in the absence of Cdk1.**

a) Bone marrow sections from *Cdk1*(lox/lox) and *Cdk1*(Δ/Δ) mice stained with Hematoxylin and eosin (H&E) or after immunodetection of Von Willebrand Factor (VWF) or phosphorylation of histone H3 (pH3). Scale bars, 50 μm (insets 20 μm). VWF signal per cell is quantified in the histogram.

b) Ploidy distribution of bone marrow CD41+ cells after DAPI staining. A representative image out of three separate experiments is shown.

c) Blood platelet levels in *Cdk1*(lox/lox) and *Cdk1*(Δ/Δ) mice.

d) Immunodetection of Cdk1 in freshly isolated megakaryocytes (CD41+ cells) from bone marrow. Megakaryocytes were stained with Hoechst and CD41+ cells were sorted according the DNA content into two populations (2C-4C) and (>4C). Vinculin was used as a loading control.

e) DNA content of CD41+ bone marrow derived >4C megakaryocytes at days 2 and 4 during polyploidization upon TPO stimulation.

f) Giemsa staining of the indicated megakaryocytes 4 days after TPO stimulation in vitro. Scale bars, 50 μm.

g) Immunodetection of Cdk1 in bone marrow derived >4C megakaryocytes after stimulation ex vivo with TPO for 3 days. Vinculin is used as a loading control. In a) and c), ns, not significant (Student's t-test).

Figure 4. Lack of Cdk1 results in endoreplicative polyploidization.

a) Cell fate of control bone marrow-derived megakaryocytes during approximately 5 days in the presence of TPO. Individual cells, stably expressing H2B-GFP (green) and Geminin-

mCherry (red), were recorded by time-lapse microscopy. The red frame stands for S-G2 phases (geminin^{high}), whereas green frames represent G1 (geminin^{low}). Endomitosis is illustrated as a black box surrounded by a purple frame.

b) Representative immunofluorescences of an individual control cell during endomitosis.

c) Quantification of geminin fluorescent intensity, nuclear volume and cell volume in individual control cells. Each line represents an individual cell and purple frames depict endomitosis. Black arrows indicate the two-fold increase in nuclear and cellular volume between two geminin^{high} phases.

d) Cell fate (similar to (a)) of individual cells derived from *Cdk1*(Δ/Δ) bone marrow derived megakaryocytes. In most cells, geminin is degraded in the absence of mitosis. Red circles indicate cell death.

e) Representative images of an individual *Cdk1*(Δ/Δ) megakaryocyte in which geminin is degraded in the absence of nuclear envelope breakdown or mitosis.

f) Quantification of the temporal profiles of geminin fluorescent intensity, nuclear volume and cell volume in *Cdk1*(Δ/Δ) megakaryocytes. Each line represents an individual cell. Black arrows highlight the two-fold increase of nuclear and cellular volume between two geminin^{high} phases even in the absence of endomitosis.

g) Schematical representation of endocycles lacking mitotic phases in the absence of Cdk1.

See also Figure S3 and S4.

Figure 5. Lack of Cdk1 and Cdk2 does not prevent megakaryocyte function despite abnormal DNA replication.

a) Representative bone marrow sections after staining with Hematoxylin and Eosin (H&E) or immunohistochemical staining for Von Willebrand Factor (VWF) and phosphorylation of H2AX (γH2AX). Scale bars, 50 μm (insets 20 μm). The quantification of the VWF signal per megakaryocyte is plotted for the indicated genotypes (ns, not significant; Student's t-test).

b) Quantification of megakaryocytes negative for γH2AX (empty box) or displaying a spotted pattern (grey boxes) or strong pan-nuclear staining (filled boxed) of γH2AX in the indicated genotypes.

c) Ploidy distribution inside the bone marrow CD41+ population after DAPI staining. Plots are representative of three different experiments. The discrete peaks corresponding to different DNA content are indicated (2C-32C). The bracket indicates the diffuse pattern of high ploidy (>8C) *Cdk1*(Δ/Δ); *Cdk2*(–/–) megakaryocytes.

d) Time-lapse microscopy of *Cdk1*(Δ/Δ); *Cdk2*(–/–) bone marrow-derived megakaryocytes after stimulation with TPO. Cells stably expressed histone H2B-GFP (red), lamin-CFP (blue) and geminin-mCherry (red). The cell increased nuclear size while maintaining its lobule organization.

e) Cell fate of multiple individual *Cdk1*(Δ/Δ); *Cdk2*(–/–) megakaryocytes. Red and green boxes represent S-G2 (geminin^{high}) or G1 (geminin^{low}) phases. Endomitosis is illustrated as a black box surrounded by a purple frame and red circles represent cell death.

f) Quantification of the temporal profiles of geminin fluorescence intensity and nuclear volume in *Cdk1*(Δ/Δ); *Cdk2*(–/–) megakaryocytes.

g) Plot representing fold increase in nuclear volume versus geminin^{high} phase length in individual megakaryocytes with the indicated genotypes.

h) A model suggesting that absence of Cdk1 and Cdk2 leads to increased ploidy by re-replication in megakaryocytes.

Figure 6. Reprogramming polyploidization rescue defects in Cdc20-deficient megakaryocytes.

a) Representative bone marrow sections from the indicated animals after staining with Hematoxylin and Eosin (H&E) or immunohistochemical staining for Von Willebrand Factor (VWF), phospho-histone H3 (pH3) or phosphorylated H2AX (γH2AX).

b) Distribution of VWF signal per megakaryocyte. Each dot represents an individual cell. n=400 cells and three mice per genotype. Student's t-test, ***, $p<0.001$.

c) Ploidy distribution inside the bone marrow CD41+ population after DAPI staining. The plot is representative from three separate experiments. Triple mutant bone marrows contain some polyploid mitotic cells, in agreement with a partial mitotic arrest imposed by Cdc20 loss, and a significant percentage of cells with intermediate levels of ploidy (Figure S5).

d) Quantification of the mitotic index in megakaryocytes of the indicated genotypes. A representative image or interphasic and mitotic megakaryocytes is shown.

e) Quantification of interphasic nuclear shape in megakaryocytes of the indicated genotypes. Cdc20-null megakaryocytes are not included since these cells are arrested in mitosis. At least 350 cells from three different animals were analyzed per genotype in d) and e) Data are mean ± SEM; ***, $p<0.001$; Student's t-test).

See also Figure S5.

Figure 7. Functional polyploidization in the absence of Cdk1 or Cdk1 and Cdk2.

a) Representative pictures of two independent DNA fiber stretch assays in bone marrow-derived megakaryocytes on day 4 after TPO stimulation. In re-replicated tracks, the green (IdU) and red (CldU) signals overlap resulting in a yellow signal. Fiber integrity was monitored with an anti-ssDNA antibody (white). The percentage of re-replicated tracks in the indicated genotypes is indicated. For each sample at least 500 measurements were performed. Data represent mean ± SEM.

b) Pro-platelet (PPT; arrows) formation in bone marrow-derived megakaryocytes analyzed 5 days after TPO stimulation. In the bottom panels, samples were stained for α-tubulin (green) and DNA (DAPI; blue).

c) The percentage of PPT-forming megakaryocytes was estimated by counting cells exhibiting 1 or more cytoplasmic protrusions with areas of platelet swellings as it is indicated by black arrows in b). At least 300 cells were analyzed per group. Data represent mean ± SEM.

d) Blood platelet levels in 8-14 week-old mice with the indicated genotypes. Each dot represents an individual animal. In a), c) and d), Student's t-test; ns, not significant; *, $p<0.5$. **, $p<0.01$; ***, $p<0.001$.

e) A model indicating the mechanisms for polyploidization in wild-type megakaryocytes (G1-S-G2-endoM) or megakaryocytes deficient in Cdk1 (G-S-G) or Cdk1; Cdk2 double mutants (re-replication in S-phase).

REFERENCES

Abe, T., Sakaue-Sawano, A., Kiyonari, H., Shioi, G., Inoue, K., Horiuchi, T., Nakao, K., Miyawaki, A., Aizawa, S., and Fujimori, T. (2013). Visualization of cell cycle in mouse embryos with Fucci2 reporter directed by Rosa26 promoter. Development *140*, 237-246.

Arias, E.E., and Walter, J.C. (2007). Strength in numbers: preventing rereplication via multiple mechanisms in eukaryotic cells. Genes Dev *21*, 497-518.

Berthet, C., Aleem, E., Coppola, V., Tessarollo, L., and Kaldis, P. (2003). Cdk2 knockout mice are viable. Curr Biol *13*, 1775-1785.

Bluteau, D., Balduini, A., Balayn, N., Currao, M., Nurden, P., Deswarte, C., Leverger, G., Noris, P., Perrotta, S., Solary, E., *et al.* (2014). Thrombocytopenia-associated mutations in the ANKRD26 regulatory region induce MAPK hyperactivation. J Clin Invest *124*, 580-591.

Broek, D., Bartlett, R., Crawford, K., and Nurse, P. (1991). Involvement of p34cdc2 in establishing the dependency of S phase on mitosis. Nature *349*, 388-393.

Calvi, B.R., Lilly, M.A., and Spradling, A.C. (1998). Cell cycle control of chorion gene amplification. Genes Dev *12*, 734-744.

Claycomb, J.M., Benasutti, M., Bosco, G., Fenger, D.D., and Orr-Weaver, T.L. (2004). Gene amplification as a developmental strategy: isolation of two developmental amplicons in Drosophila. Dev Cell *6*, 145-155.

Dahmann, C., Diffley, J.F., and Nasmyth, K.A. (1995). S-phase-promoting cyclin-dependent kinases prevent re-replication by inhibiting the transition of replication origins to a pre-replicative state. Curr Biol *5*, 1257-1269.

Davoli, T., and de Lange, T. (2011). The causes and consequences of polyploidy in normal development and cancer. Annu Rev Cell Dev Biol *27*, 585-610.

Dieguez-Hurtado, R., Martin, J., Martinez-Corral, I., Martinez, M.D., Megias, D., Olmeda, D., and Ortega, S. (2011). A Cre-reporter transgenic mouse expressing the far-red fluorescent protein Katushka. Genesis *49*, 36-45.

Diril, M.K., Ratnacaram, C.K., Padmakumar, V.C., Du, T., Wasser, M., Coppola, V., Tessarollo, L., and Kaldis, P. (2012). Cyclin-dependent kinase 1 (Cdk1) is essential for cell division and suppression of DNA re-replication but not for liver regeneration. Proc Natl Acad Sci U S A *109*, 3826-3831.

Dorn, E.S., Chastain, P.D., 2nd, Hall, J.R., and Cook, J.G. (2009). Analysis of re-replication from deregulated origin licensing by DNA fiber spreading. Nucleic Acids Res *37*, 60-69.

Eckly, A., Heijnen, H., Pertuy, F., Geerts, W., Proamer, F., Rinckel, J.Y., Leon, C., Lanza, F., and Gachet, C. (2014). Biogenesis of the demarcation membrane system (DMS) in megakaryocytes. Blood *123*, 921-930.

Edgar, B.A., and Orr-Weaver, T.L. (2001). Endoreplication cell cycles: more for less. Cell *105*, 297-306.

Edgar, B.A., Zielke, N., and Gutierrez, C. (2014). Endocycles: a recurrent evolutionary innovation for post-mitotic cell growth. Nat Rev Mol Cell Biol *15*, 197-210.

Fernandez-Miranda, G., Trakala, M., Martin, J., Escobar, B., Gonzalez, A., Ghyselinck, N.B., Ortega, S., Canamero, M., Perez de Castro, I., and Malumbres, M. (2011). Genetic disruption of

aurora B uncovers an essential role for aurora C during early mammalian development. Development *138*, 2661-2672.

Gao, Y., Smith, E., Ker, E., Campbell, P., Cheng, E.C., Zou, S., Lin, S., Wang, L., Halene, S., and Krause, D.S. (2012). Role of RhoA-specific guanine exchange factors in regulation of endomitosis in megakaryocytes. Dev Cell *22*, 573-584.

Garcia-Higuera, I., Manchado, E., Dubus, P., Canamero, M., Mendez, J., Moreno, S., and Malumbres, M. (2008). Genomic stability and tumour suppression by the APC/C cofactor Cdh1. Nat Cell Biol *10*, 802-811.

Geddis, A.E., Fox, N.E., Tkachenko, E., and Kaushansky, K. (2007). Endomitotic megakaryocytes that form a bipolar spindle exhibit cleavage furrow ingression followed by furrow regression. Cell Cycle *6*, 455-460.

Gupta, S. (2000). Hepatic polyploidy and liver growth control. Semin Cancer Biol *10*, 161-171.

Hassel, C., Zhang, B., Dixon, M., and Calvi, B.R. (2014). Induction of endocycles represses apoptosis independently of differentiation and predisposes cells to genome instability. Development *141*, 112-123.

Hochegger, H., Dejsuphong, D., Sonoda, E., Saberi, A., Rajendra, E., Kirk, J., Hunt, T., and Takeda, S. (2007). An essential role for Cdk1 in S phase control is revealed via chemical genetics in vertebrate cells. J Cell Biol *178*, 257-268.

Josefsson, E.C., James, C., Henley, K.J., Debrincat, M.A., Rogers, K.L., Dowling, M.R., White, M.J., Kruse, E.A., Lane, R.M., Ellis, S., *et al.* (2011). Megakaryocytes possess a functional intrinsic apoptosis pathway that must be restrained to survive and produce platelets. J Exp Med *208*, 2017-2031.

Kaushansky, K. (2008). Historical review: megakaryopoiesis and thrombopoiesis. Blood *111*, 981-986.

Krause, D.S., and Crispino, J.D. (2013). Molecular pathways: induction of polyploidy as a novel differentiation therapy for leukemia. Clin Cancer Res *19*, 6084-6088.

Lordier, L., Bluteau, D., Jalil, A., Legrand, C., Pan, J., Rameau, P., Jouni, D., Bluteau, O., Mercher, T., Leon, C., *et al.* (2012). RUNX1-induced silencing of non-muscle myosin heavy chain IIB contributes to megakaryocyte polyploidization. Nat Commun *3*, 717.

Lordier, L., Chang, Y., Jalil, A., Aurade, F., Garcon, L., Lecluse, Y., Larbret, F., Kawashima, T., Kitamura, T., Larghero, J., *et al.* (2010). Aurora B is dispensable for megakaryocyte polyploidization, but contributes to the endomitotic process. Blood *116*, 2345-2355.

Lordier, L., Jalil, A., Aurade, F., Larbret, F., Larghero, J., Debili, N., Vainchenker, W., and Chang, Y. (2008). Megakaryocyte endomitosis is a failure of late cytokinesis related to defects in the contractile ring and Rho/Rock signaling. Blood *112*, 3164-3174.

Machlus, K.R., and Italiano, J.E., Jr. (2013). The incredible journey: From megakaryocyte development to platelet formation. J Cell Biol *201*, 785-796.

Malumbres, M., and Barbacid, M. (2009). Cell cycle, CDKs and cancer: a changing paradigm. Nat Rev Cancer *9*, 153-166.

Malumbres, M., Harlow, E., Hunt, T., Hunter, T., Lahti, J.M., Manning, G., Morgan, D.O., Tsai, L.H., and Wolgemuth, D.J. (2009). Cyclin-dependent kinases: a family portrait. Nat Cell Biol *11*, 1275-1276.

Manchado, E., Guillamot, M., de Carcer, G., Eguren, M., Trickey, M., Garcia-Higuera, I., Moreno, S., Yamano, H., Canamero, M., and Malumbres, M. (2010). Targeting mitotic exit leads to tumor regression in vivo: Modulation by Cdk1, Mastl, and the PP2A/B55alpha,delta phosphatase. Cancer Cell *18*, 641-654.

Mehrotra, S., Maqbool, S.B., Kolpakas, A., Murnen, K., and Calvi, B.R. (2008). Endocycling cells do not apoptose in response to DNA rereplication genotoxic stress. Genes Dev *22*, 3158-3171.

Moore, J.D., Kirk, J.A., and Hunt, T. (2003). Unmasking the S-phase-promoting potential of cyclin B1. Science *300*, 987-990.

Neelsen, K.J., Zanini, I.M., Mijic, S., Herrador, R., Zellweger, R., Ray Chaudhuri, A., Creavin, K.D., Blow, J.J., and Lopes, M. (2013). Deregulated origin licensing leads to chromosomal breaks by rereplication of a gapped DNA template. Genes Dev *27*, 2537-2542.

Nezi, L., and Musacchio, A. (2009). Sister chromatid tension and the spindle assembly checkpoint. Curr Opin Cell Biol *21*, 785-795.

Ortega, S., Prieto, I., Odajima, J., Martin, A., Dubus, P., Sotillo, R., Barbero, J.L., Malumbres, M., and Barbacid, M. (2003). Cyclin-dependent kinase 2 is essential for meiosis but not for mitotic cell division in mice. Nat Genet *35*, 25-31.

Pandit, S.K., Westendorp, B., and de Bruin, A. (2013). Physiological significance of polyploidization in mammalian cells. Trends Cell Biol *23*, 556-566.

Papadantonakis, N., Makitalo, M., McCrann, D.J., Liu, K., Nguyen, H.G., Martin, G., Patel-Hett, S., Italiano, J.E., and Ravid, K. (2008). Direct visualization of the endomitotic cell cycle in living megakaryocytes: differential patterns in low and high ploidy cells. Cell Cycle *7*, 2352-2356.

Peters, J.M. (2006). The anaphase promoting complex/cyclosome: a machine designed to destroy. Nat Rev Mol Cell Biol *7*, 644-656.

Ravid, K., Lu, J., Zimmet, J.M., and Jones, M.R. (2002). Roads to polyploidy: the megakaryocyte example. J Cell Physiol *190*, 7-20.

Sakaue-Sawano, A., Hoshida, T., Yo, M., Takahashi, R., Ohtawa, K., Arai, T., Takahashi, E., Noda, S., Miyoshi, H., and Miyawaki, A. (2013). Visualizing developmentally programmed endoreplication in mammals using ubiquitin oscillators. Development *140*, 4624-4632.

Sakaue-Sawano, A., Kurokawa, H., Morimura, T., Hanyu, A., Hama, H., Osawa, H., Kashiwagi, S., Fukami, K., Miyata, T., Miyoshi, H., *et al.* (2008). Visualizing spatiotemporal dynamics of multicellular cell-cycle progression. Cell *132*, 487-498.

Santamaria, D., Barriere, C., Cerqueira, A., Hunt, S., Tardy, C., Newton, K., Caceres, J.F., Dubus, P., Malumbres, M., and Barbacid, M. (2007). Cdk1 is sufficient to drive the mammalian cell cycle. Nature *448*, 811-815.

Sher, N., Von Stetina, J.R., Bell, G.W., Matsuura, S., Ravid, K., and Orr-Weaver, T.L. (2013). Fundamental differences in endoreplication in mammals and Drosophila revealed by analysis of endocycling and endomitotic cells. Proc Natl Acad Sci U S A *110*, 9368-9373.

Thon, J.N., and Italiano, J.E., Jr. (2012). Does size matter in platelet production? Blood *120*, 1552-1561.

Tiedt, R., Schomber, T., Hao-Shen, H., and Skoda, R.C. (2007). Pf4-Cre transgenic mice allow the generation of lineage-restricted gene knockouts for studying megakaryocyte and platelet function in vivo. Blood *109*, 1503-1506.

Trakala, M., Fernandez-Miranda, G., Perez de Castro, I., Heeschen, C., and Malumbres, M. (2013). Aurora B prevents delayed DNA replication and premature mitotic exit by repressing p21(Cip1). Cell Cycle *12*, 1030-1041.

Ullah, Z., Kohn, M.J., Yagi, R., Vassilev, L.T., and DePamphilis, M.L. (2008). Differentiation of trophoblast stem cells into giant cells is triggered by p57/Kip2 inhibition of CDK1 activity. Genes Dev *22*, 3024-3036.

Vitrat, N., Cohen-Solal, K., Pique, C., Le Couedic, J.P., Norol, F., Larsen, A.K., Katz, A., Vainchenker, W., and Debili, N. (1998). Endomitosis of human megakaryocytes are due to abortive mitosis. Blood *91*, 3711-3723.

Wen, Q., Goldenson, B., Silver, S.J., Schenone, M., Dancik, V., Huang, Z., Wang, L.Z., Lewis, T.A., An, W.F., Li, X., *et al.* (2012). Identification of regulators of polyploidization presents therapeutic targets for treatment of AMKL. Cell *150*, 575-589.

Wen, Q., Leung, C., Huang, Z., Small, S., Reddi, A.L., Licht, J.D., and Crispino, J.D. (2009). Survivin is not required for the endomitotic cell cycle of megakaryocytes. Blood *114*, 153-156.

Zhang, Y., Wang, Z., and Ravid, K. (1996). The cell cycle in polyploid megakaryocytes is associated with reduced activity of cyclin B1-dependent cdc2 kinase. J Biol Chem *271*, 4266-4272.

Zhu, Y. (2004). A model for CDK2 in maintaining genomic stability. Cell Cycle *3*, 1358-1362.

Zielke, N., Edgar, B.A., and DePamphilis, M.L. (2013). Endoreplication. Cold Spring Harb Perspect Biol *5*, a012948.

Zimmet, J., and Ravid, K. (2000). Polyploidy: occurrence in nature, mechanisms, and significance for the megakaryocyte-platelet system. Exp Hematol *28*, 3-16.

Figure

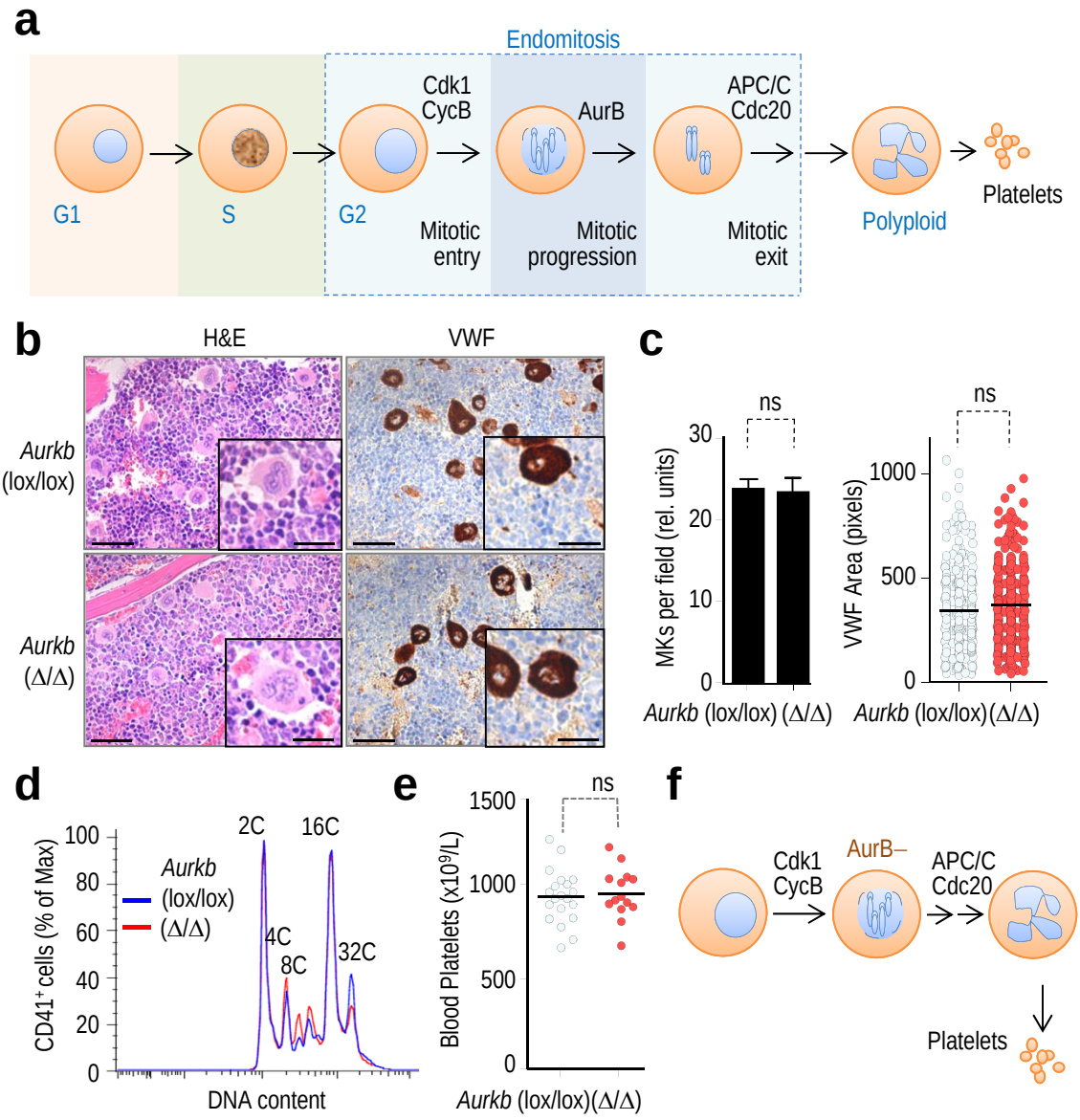

Figure 1

Figure

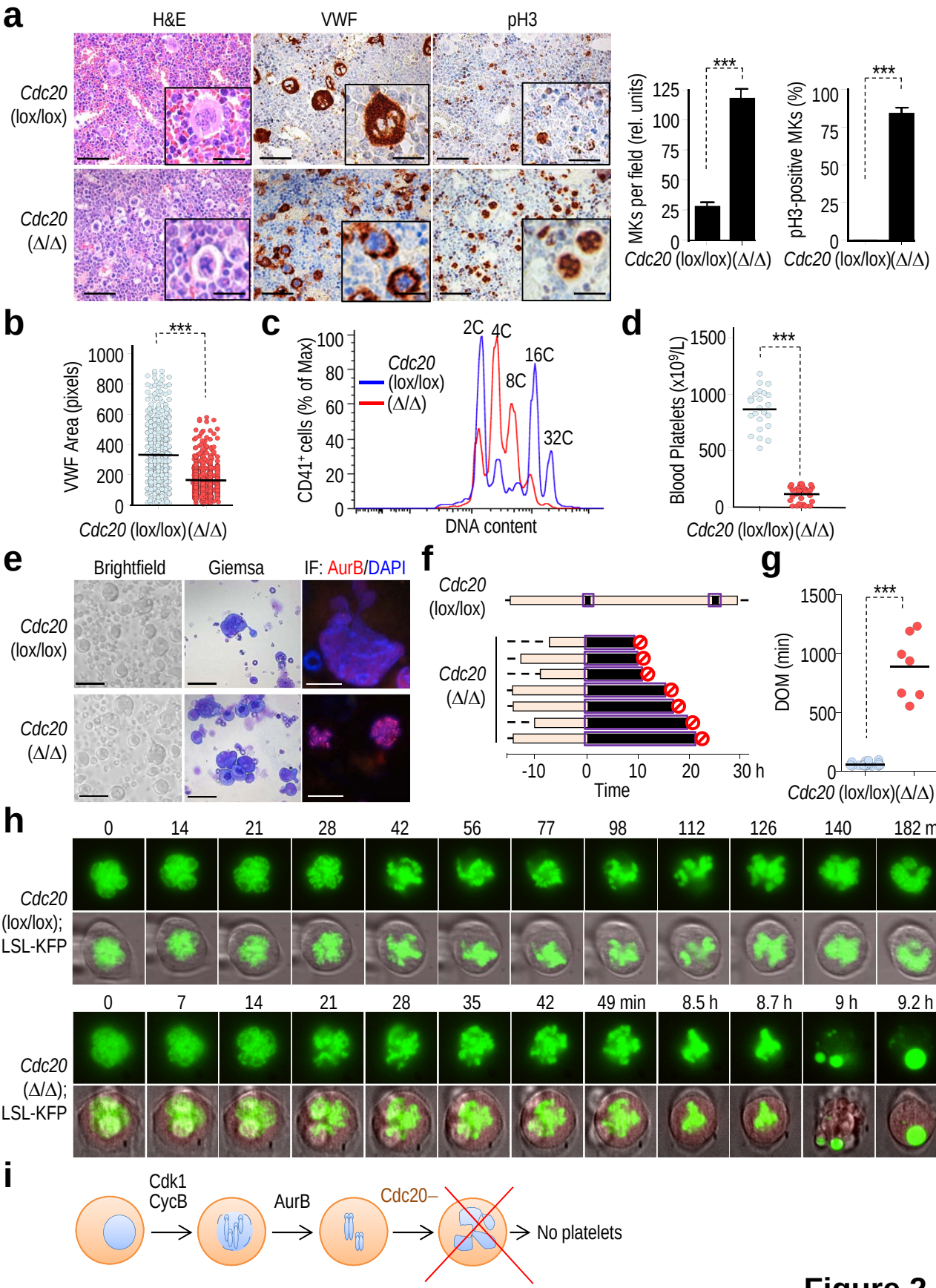

Figure 2

Figure

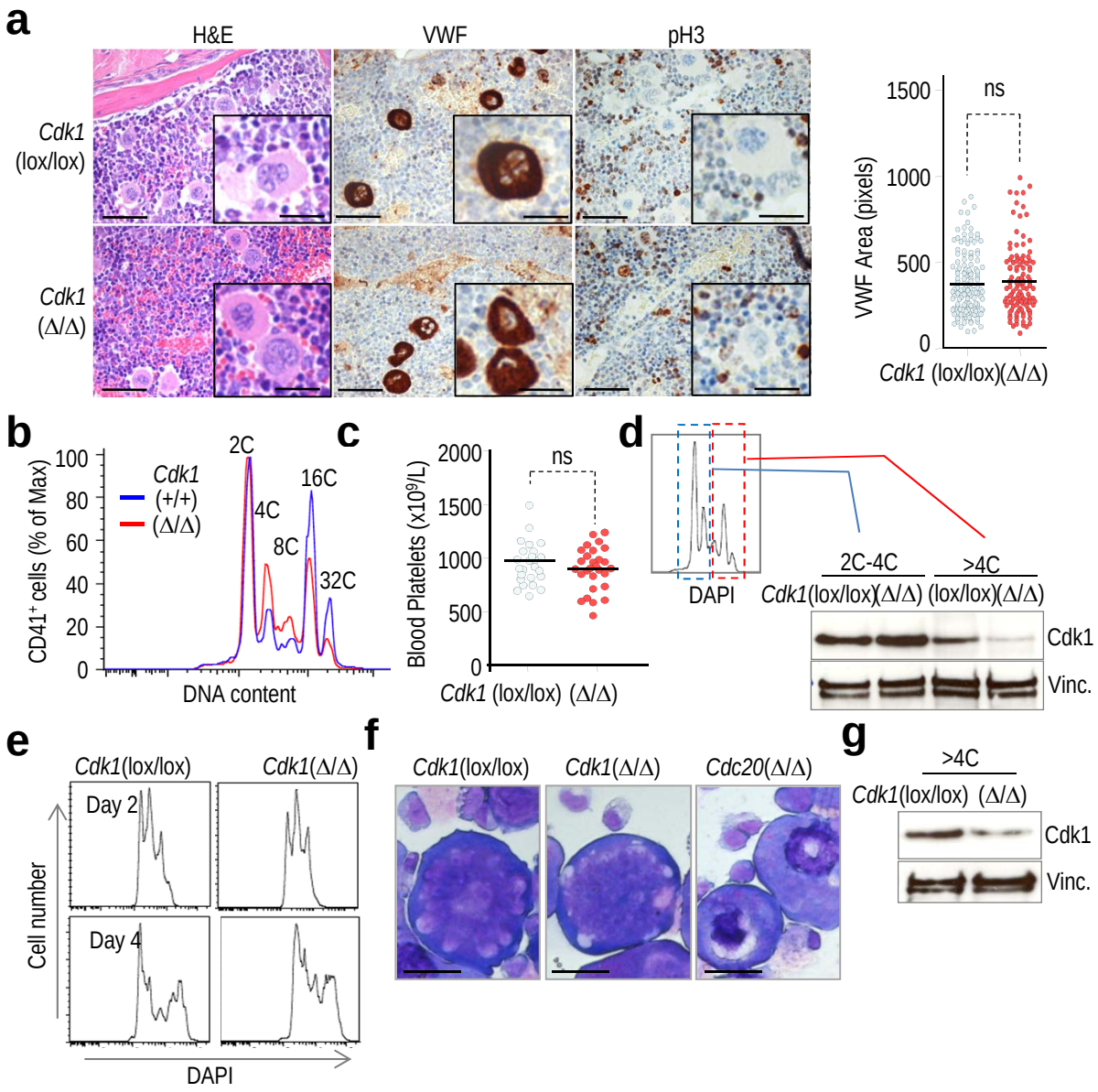

Figure 3

Figure

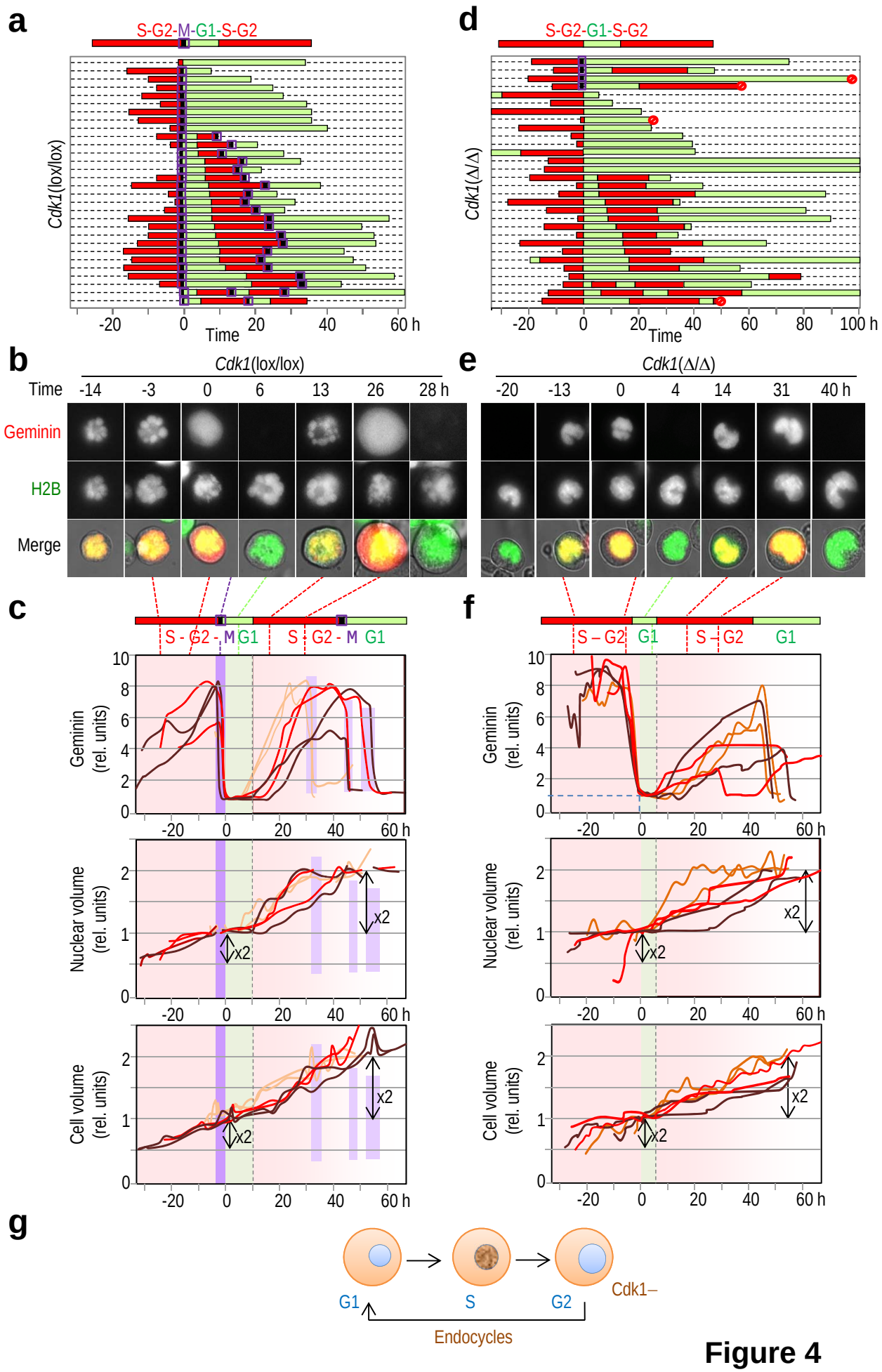

Figure 4

Figure

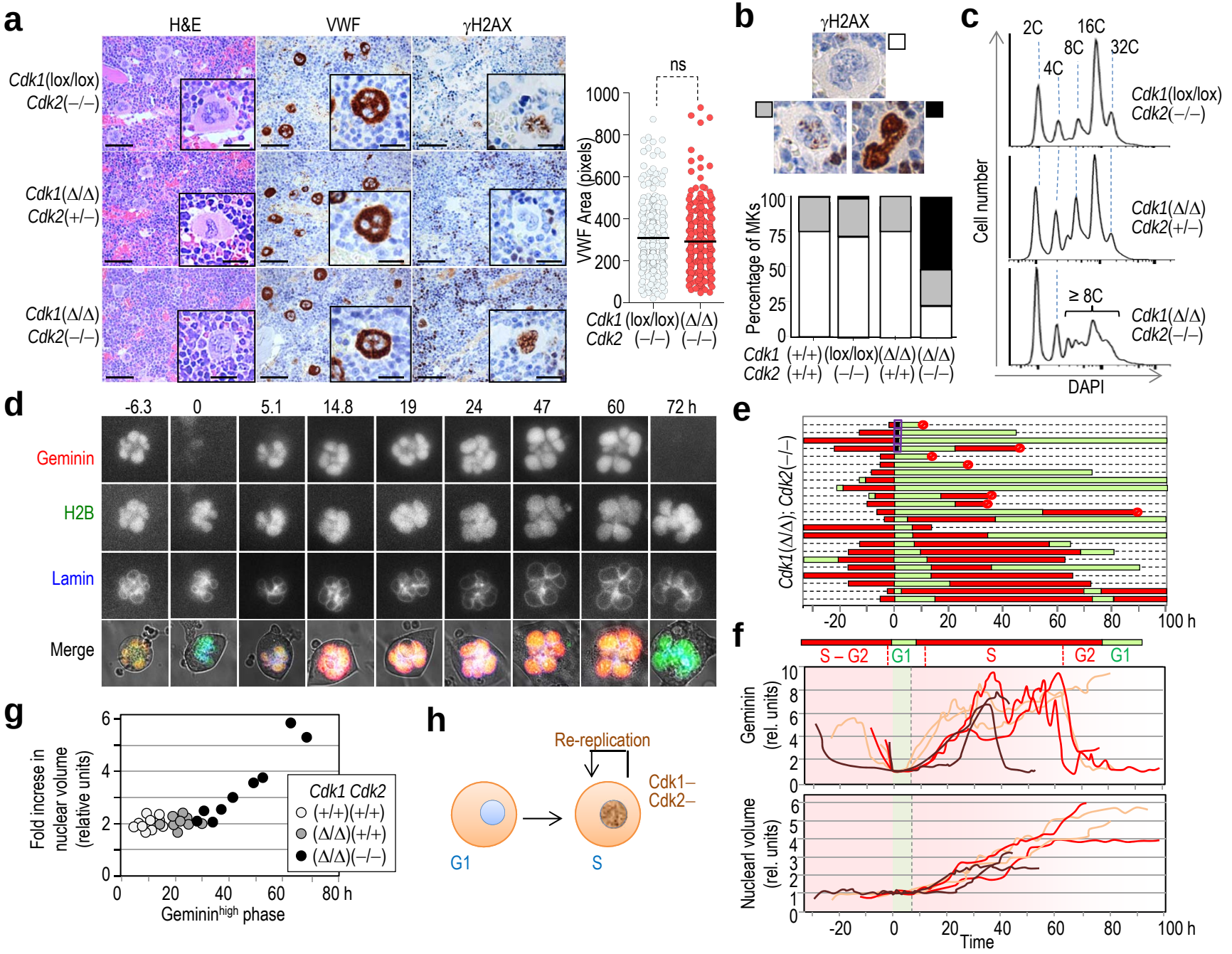

Figure 5

Figure

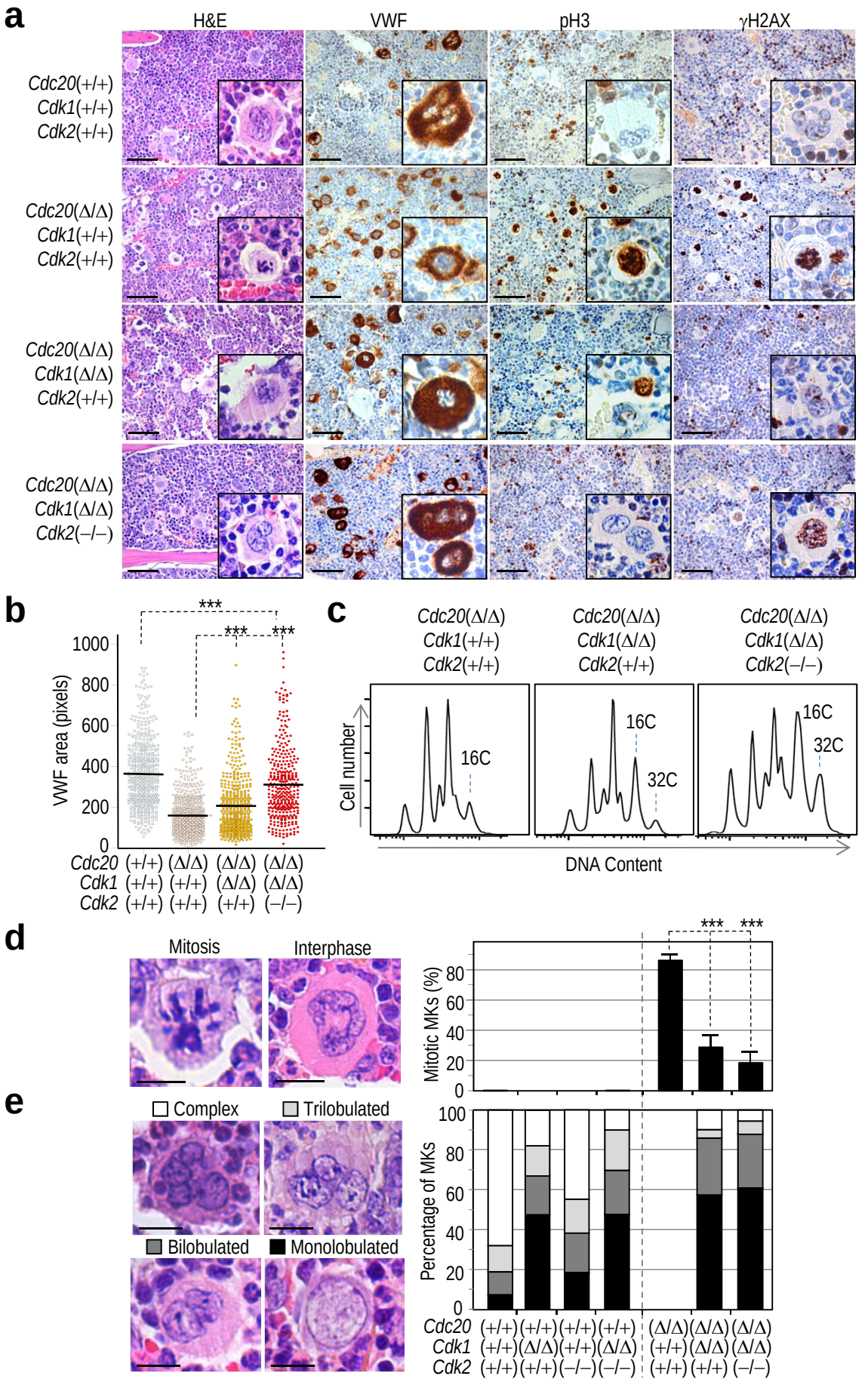

Figure 6

Figure

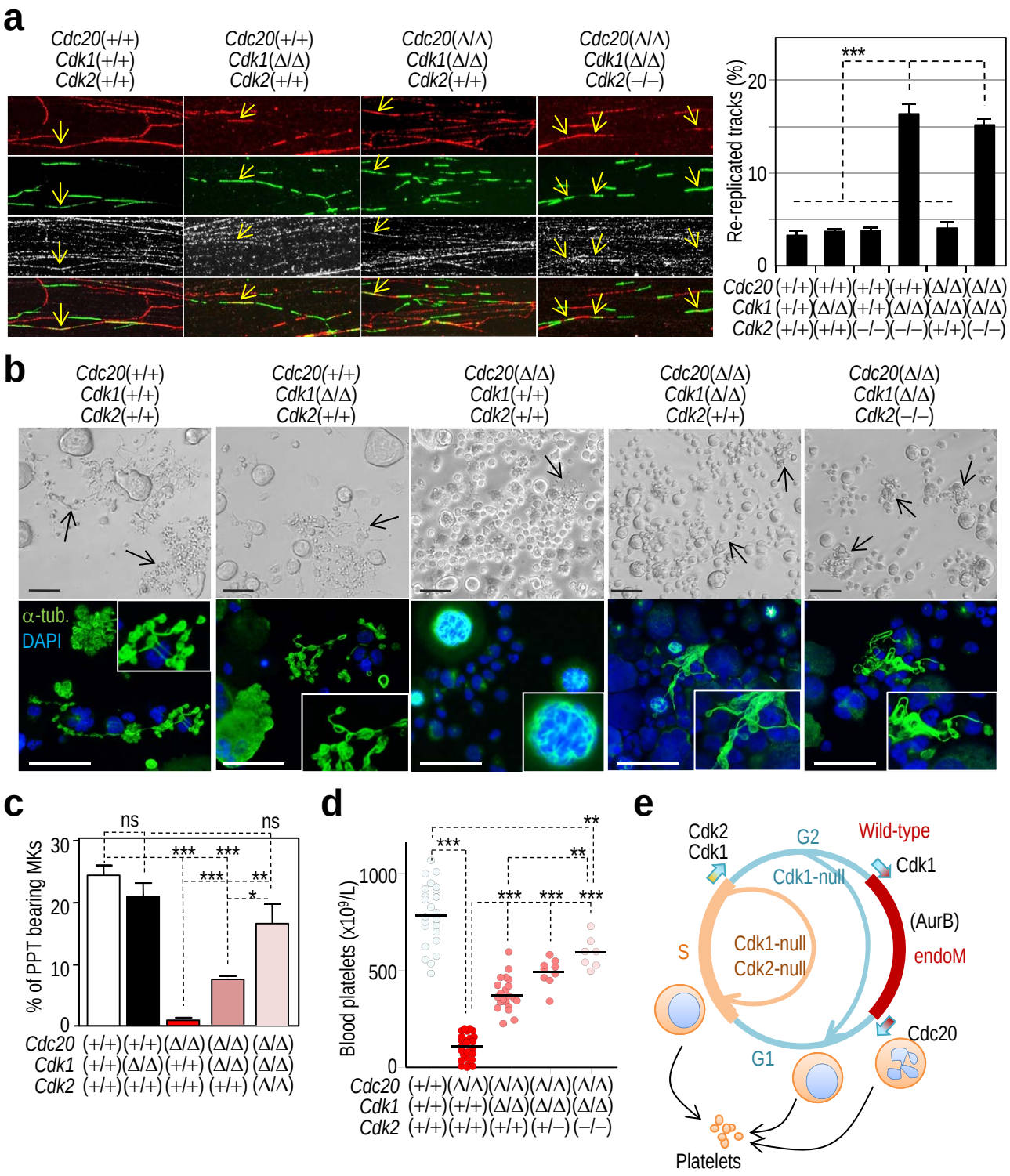

Figure 7

Supplemental Inventory

Supplemental Figures

Figure S1. Genetic tools for megakaryocyte-specific ablation of cell cycle regulators. Schematic representation of Pf4-Cre mediated gene ablation and the LSL-Katushka reporter. Consequences of Aurora B ablation in megakaryocytes. Related to Figure 1.

Figure S2. Analysis of hematopoietic progenitors as a consequence of severe thrombocytopenia in *Cdc20*(Δ/Δ) mice. Related to Figure 2.

Figure S3. Time-lapse microscopy of endomitotic polyploidization in megakaryocytes after in vitro differentiation with TPO. Related to Figure 4.

Figure S4. Time-lapse microscopy of endocycling in Cdk1-deficient cells after in vitro differentiation with TPO. Related to Figure 4.

Figure S5. Polyploidization and cell fate of megakaryocytes with Cdk1 and Cdk2-mutant alleles in a Cdc20-null background. Related to Figure 6.

Supplemental Experimental Procedures

Supplemental References

Supplementary Figures

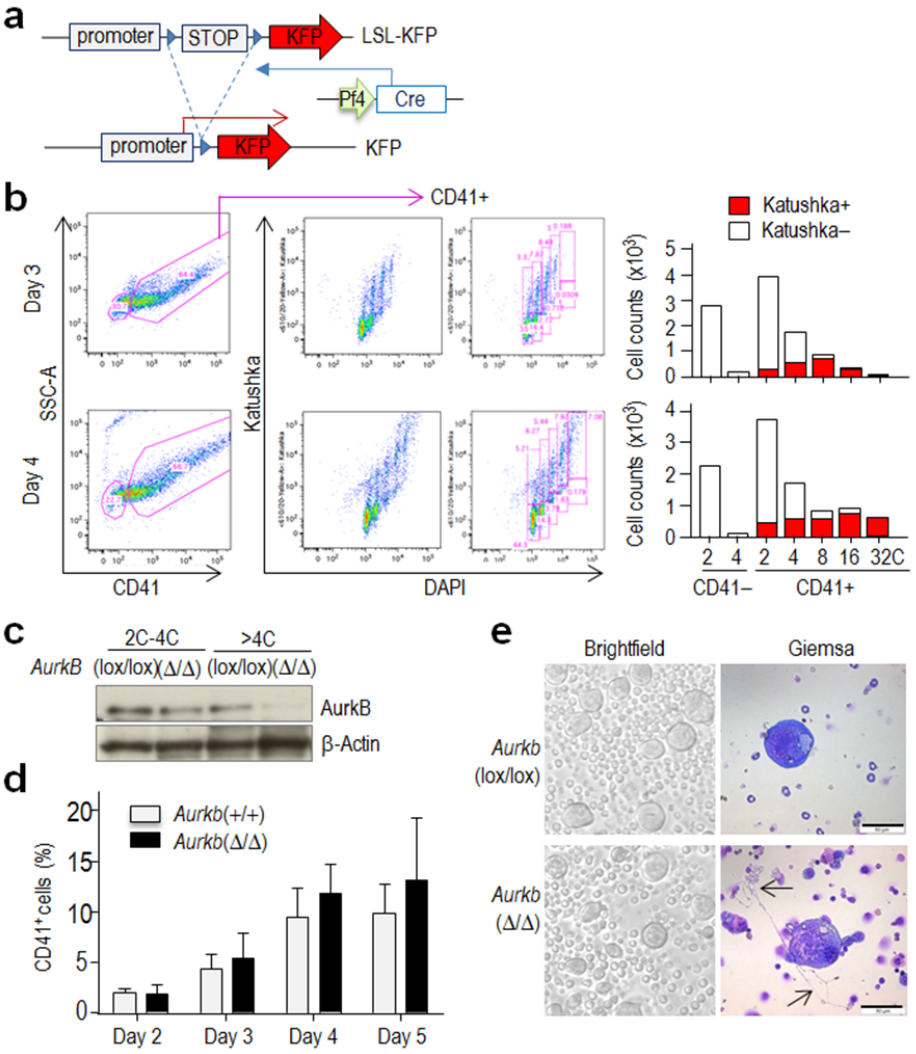

Figure S1. Genetic tools for megakaryocyte-specific ablation of cell cycle regulators (related to Figure 1). a) Schematic representation of the LoxP-STOP-LoxP (LSL)- Katushka-fluorescent protein (KFP) reporter. b) Validation of Pf4-Cre activity using the LSL-KFP reporter in polyploid megakaryocytes. Bone marrow progenitors (lin-) carrying the Pf4-Cre and LSL-KFP alleles were stimulated in vitro in the presence of TPO and Cre activity was monitored by analyzing KFP. As shown in the histograms, three or four days after TPO treatment, most polyploid (≥8C) megakaryocytes express KFP as a consequence of the Cre-dependent excision of the STOP cassette, wheras less than half of the 4C cells and a very reduced percentage of 2C cells are positive for this marker. c) Immunodetection of Aurora B in low ploidy (2C-4C) or high ploidy (≥4C) megakaryocytes (CD41-positive cells) in the bone marrow from the indicated genotypes. β-actin was used as a loading control. d) The cumulative percentage of CD41+ cells (mean ± SEM) is similar in *Aurkb*(Δ/Δ) and *Aurkb*(+/+) cultures (P>0.05; Student's t-test) on days 2-5 after TPO stimulation of E13.5 fetal liver cells. e) Representative images of fetal liver-derived megakaryocytes 5 days after stimulation with TPO showing similar number and appearance of large megakaryocytes. Pro-platelet formation occurs in the absence of Aurora B as indicated by arrows in right lower panel. Scale bars, 50 μm.

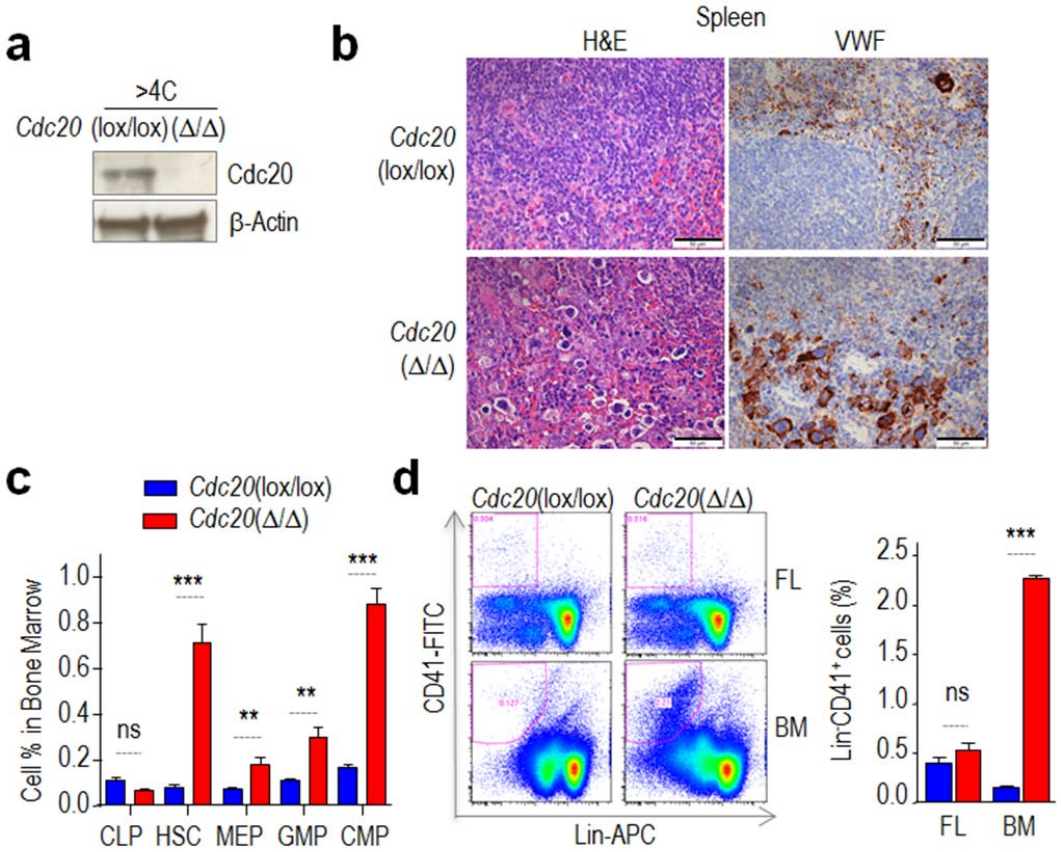

Figure S2. High levels of hematopoietic progenitors as a consequence of severe thrombocytopenia in *Cdc20*(Δ/Δ) mice (related to Figure 2). a) Immunodetection of Cdc20 in high ploidy (≥4C) megakaryocytes (CD41-positive cells) in the bone marrow from the indicated genotypes. β-actin was used as a loading control. b) Hematoxylin and eosin (H&E) staining and immunohistochemical staining for Von Willebrand Factor (VWF) in spleen sections from in 8-12 week-old animals with the indicated genotypes. Scale bars, 50 μm. c) Percentage of hematopoietic progenitors from the bone marrow of *Cdc20*(Δ/Δ) and control in 8-12 week-old mice after FACS analysis with specific markers (see Extended Experimental Protocols). HSCs, Hematopoetic stem cells; CLPs, common lympoid progenitors; CMPs, Common myeloid progenitors; MEPs, megakaryocyte-erythrocyte progenitors; GMPs, granulocyte-macrophage progenitors. n=5 mice per group d) Representative data and quantification of the CD41+ population after FACS analysis of total fetal liver (FL) cells from E12.5 embryos or cells from the bone marrow (BM) of 8 week-old mice. n=3 mice per group. All graphs show mean ± SEM. Statistics were performed by Student's t-test; ns, not significant; **, p<0.01; ***, p<0.001.

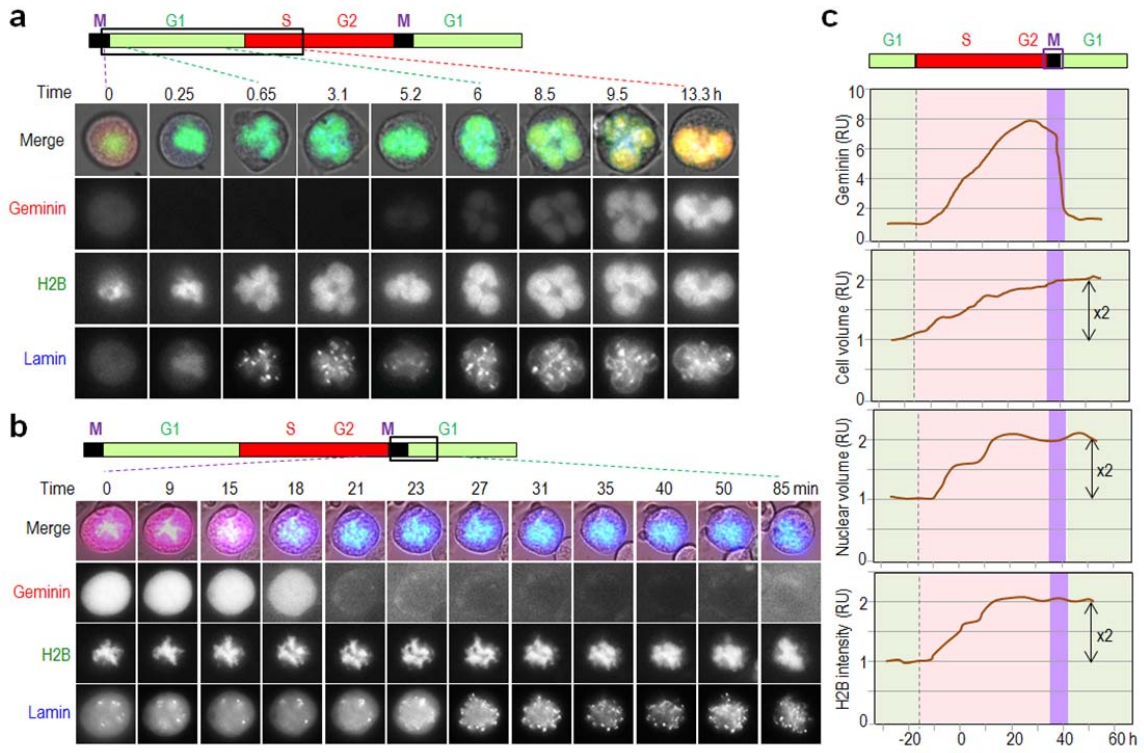

Figure S3. Time-lapse microscopy of endomitotic polyploidization in vitro (related to Figure 4). Time-lapse microscopy of bone marrow derived megakaryocytes stably expressing histone-GFP (H2B-GFP; green), lamin-CFP (blue) and geminin-mCherry (Red). a) Representative pictures of an individual cell during the G1-S transition. Time=0 represents the exit from endomitosis characterized by degradation of geminin (red), decondensation of chromatin (green) and nuclear envelope reformation (blue). During G1-phase cells are negative for geminin and start to express it upon G1-S transition. During S-phase the increase in nuclear volume can be appreciated. b) Representative images of an individual cell during endomitosis. Endomitosis is characterized by chromatin condensation and the absence of nuclear envelope, resulting in the pancellular distribution of geminin, which is exclusively nuclear during interphase. In late stages of endomitosis, geminin is degraded and nuclear envelope reforms and chromatin decondenses. c) Plots showing the relative units of geminin-mCherry mean fluorescent intensity, H2B-GFP mean fluorescent intensity, and nuclear and cellular volume during the endomitotic cell cycle in a representative megakaryocyte. The purple frame depicts endomitosis (M).

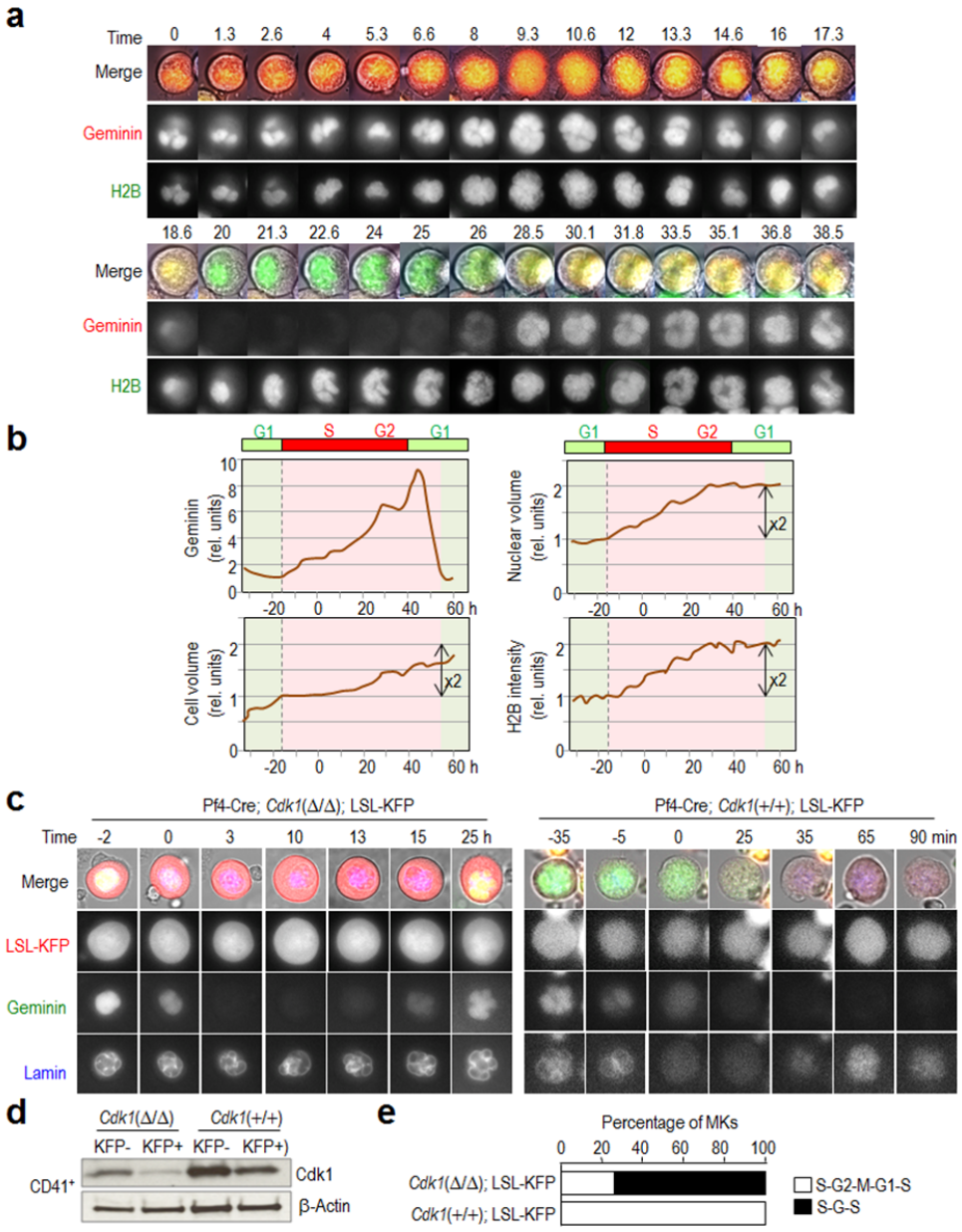

Figure S4. Time-lapse microscopy of endocycling Cdk1-deficient cells in vitro (related to Figure 4). a) Time-lapse microscopy of bone marrow derived *Cdk1*(Δ/Δ) megakaryocytes stably expressing histone-GFP (H2B-GFP; green) and geminin-mCherry (Red). Time=0 was arbitrarily set. Geminin is degraded (at ~17-18 h) in the absence of mitosis; i.e. without nuclear envelope breakdown (as detected by the absence of nuclear-to-cytoplasmic redistribution of geminin, and absence of DNA condensation). During G1 cells are negative for geminin and start to express it at the G1-S transition. b) Plots showing the relative units of geminin-mCherry mean fluorescent intensity, H2B-GFP mean fluorescent intensity, and nuclear and cellular volume during the endoreplication process in a representative *Cdk1*(Δ/Δ) megakaryocyte. c) Time-lapse microscopy of megakaryocytes expressing geminin (green), lamin (blue) and KFP (red). d) Immunodetection of Cdk1 in CD41-positive cells isolated from the bone marrow of Pf4-Cre; *Cdk1*(Δ/Δ); LSL-KFP or Pf4-Cre; *Cdk1*(+/+); LSL-KFP animals. KFP-positive (+) or negative (-) cells were isolated by flow cytometry. β-actin was used as a loading control. e) Quantification from (c); most KFP-positive Cdk1-null megakaryocytes (n=12) undergo S-G-S (endocycles) whereas all (n=14) KFP-positive control megakaryocytes display typical endomitotic cycles (M, endomitosis).

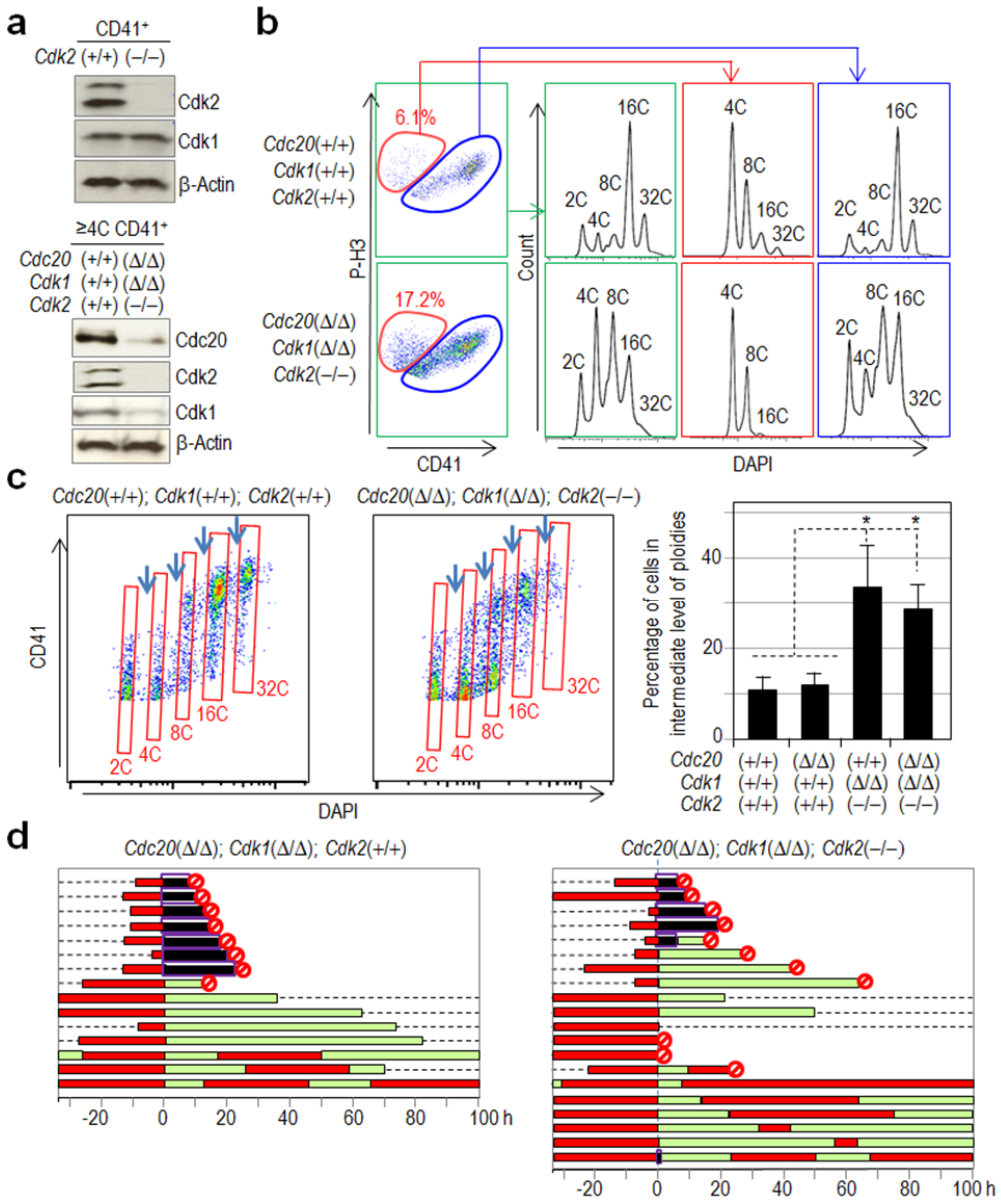

Figure S5. Polyploidization and cell fate of megakaryocytes with Cdk1 and Cdk2-mutant alleles in a Cdc20-null background (related to Figure 6). a) Immunodetection of the indicated proteins in total megakaryocytes (CD41-positive cells) or high ploidy (≥4C) CD41-positive cells from the bone marrow. β-actin was used as a loading control. b) Analysis of mitosis (phospho-histone H3; P-H3 signal) in CD41+ bone marrow cells from wild-type or *Cdc20*(Δ/Δ); *Cdk1*(Δ/Δ); *Cdk2*(–/–) mice. The ploidy profiles of the whole CD41+ population (green), P-H3-positive (red) or P-H3-negative (blue) cells are shown. c) Quantification of cells with intermediate levels of ploidy (arrows). Three animals per genotype were analyzed. *, p<0.5; Student's t-test. d) Cell fate of individual *Cdc20*(Δ/Δ); *Cdk1*(Δ/Δ) [left] or *Cdc20*(Δ/Δ); *Cdk1*(Δ/Δ); *Cdk2*(–/–) [right] bone marrow-derived megakaryocytes recorded by time-lapse microscopy. Cells stably expressed histone H2B-GFP, lamin-CFP and geminin-mCherry. Red and green boxes represent S-G2 (geminin^{high}) or G1 (geminin^{low}) phases, respectively. Endomitosis, prolonged in all cases as a consequence of lack of Cdc20, is illustrated as a black box surrounded by a purple frame and red circles represent cell death.

Supplemental Experimental Procedures

Mouse colony and histological analysis

For genotyping the different alleles from the mouse models tail DNA was isolated from 3-4-week old mice and PCR amplification reactions were performed using the oligonucleotides described in the original manuscripts (Dieguez-Hurtado et al., 2011; Fernandez-Miranda et al., 2011; Manchado et al., 2010; Ortega et al., 2003; Tiedt et al., 2007) Cdk1 mutant mice were genotyped using oligonucleotides Fw: 5'-GAGATGTAGGATGACTCAGTG-3' and Rv: 5'-TAGCTTATCTACCTCAGCCTG-3', which generate amplification bands of 650 bp (wild-type allele) or 800 bp (mutant allele). The following amplification conditions were used: 94ºC during 4 minutes followed by 35 cycles of DNA denaturalization at 94ºC during 30 seconds, primer annealing at 60ºC during 30 seconds and polymerase extension at 72ºC during 60 seconds ending with a single elongation cycle of 7 minutes at 72ºC. For histology sections, sterna and spleens were fixed overnight in 4% formalin. Sterna were then decalcified in Decalcifier I solution (Surgipath) for 2 hours. Samples were dehydrated in 70% ethanol and processed by the Histopathology Facility Unit at CNIO for 3-5 μm longitudinal paraffin sections, hematoxylin and eosin staining, or immunohistochemistry.

Isolation of bone marrow or fetal liver cells and cytometry

For bone marrow derived megakaryocytes, the tibia and femur were isolated from 8-12 week old mice and bone marrow was flushed out by the addition of ice-cold PBS buffer (PBS, 0.5% BSA, 5mM EDTA) through the lumen of the bone. Marrow was mechanically disrupted to achieve single cell suspension followed by filtering through a 40μm nylon strainer to remove bone debris and subsequently subjected to erythrocyte lysis. For red blood cell lysis the bone marrow cell pellet from 1 mouse was resuspended in 1 ml of ACK lysis buffer (150 mM ammonium chloride, 1 mM potassium bicarbonate, 0.1 mM EDTA) and incubated for 1.5 min on ice. The lysis was stopped by the addition of 10 ml PBS buffer and cells were centrifuged at 200*g* for 10 min. Cells were counted and subjected either directly to surface antigen staining for flow cytometry analysis or to lineage depletion with the Miltenyi MACS (magnetic cell shorting) Hematopoietic Progenitor (Stem) Cell Enrichment Set, according to manufacturer's protocol. For fetal liver derived megakaryocytes, cells were obtained from whole livers recovered from mouse fetuses between embryonic days 12.5 and 13.5. Single-cell suspensions were prepared by successive passage through 19-, 22-, and 25-gauge needles.

To determine mouse bone marrow hematopoietic stem cells (HSC; Lin^- $IL7R^-$ $c\text{-}kit^+$ Sca^+), common lymphoid progenitors (CLP; Lin^- $IL7R^+$ $c\text{-}kit^+$ Sca^+), common myeloid progenitors (CMP; Lin^- $IL7R^-$ $c\text{-}kit^+$ Sca^- $CD34^+$, $Fc\gamma R^{low}$), megakaryocyte, erythroid progenitors (MEP; Lin^- $IL7R^-$ $c\text{-}kit^+$ Sca^- $CD34^-$, $Fc\gamma R^{low}$), granulocyte, macrophage progenitors (GMP; Lin^- $IL7R^-$ $c\text{-}kit^+$ Sca^- $CD34^+$, $Fc\gamma R^{high}$), and megakaryocyte progenitors (Lin^- $CD41^+$) cells, freshly obtained BM cells were stained with phycoerythrin (PE) anti-CD34 (BD Biosciences), Alexa Fluor 488 anti- IL7Ra, peridinin chlorophyll Protein Cyanin 5.5 (PerCP-Cy 5.5 anti–Sca-1, allophycocyanin-H7 (APC-H7) anti-cKit (BD

Biosciences), phycoerythrin-cyanin 7 (PE-Cy7) anti-FcγR (BD Biosciences) and allophycocyanin (APC) -labeled lineage cell detection cocktail (BD Biosciences). Flow cytometric analysis was performed with a FACS-Canto flow cytometer or a LSRII flow cytometer (BD Biosciences) and FlowJo Version 8.8.7 software (TreeStar).

Virus preparation

For preparation of viruses, low passage 293T cells were transfected with the vector of interest and the three packaging vectors expressing gag, pol and rev proteins necessary for virion production as well the envelope protein vsvg (Tiscornia et al., 2006). 48 h post transfection supernatants containing viruses were collected and concentrated by centrigufation at 19.400 rpm for 2 hours at 20 ºC. Viral pellets were resuspended in 1x HBSS. This viral preparation is of in vitro grade quality. For retroviruses, 293T cells were transfected with the vector of interest and the packaging vector PCL-Eco. Supernatants were collected and 48 hours post transfection. Packaging vectors are a gift from Dr. Verma´s lab. Transduction of primary megakaryocytes and Lin- bone marrow cells were performed by adding 10 μl of concentrated virus (stock 10^9 viral particles per mL) per million of cells (MOI 10) for 12 h.

Supplemental References

Tiscornia, G., Singer, O., and Verma, I.M. (2006). Production and purification of lentiviral vectors. Nat Protoc 1, 241-245.